Global Ecology and Biogeography

Range-wide variation in local adaptation and phenotypic plasticity of fitness-related traits in Fagus sylvatica and their implications under climate change

SCHOLARONE™
Manuscripts

1 **Range-wide variation in local adaptation and phenotypic plasticity of**

2 **fitness-related traits in *Fagus sylvatica* and their implications under**

3 **climate change**

4 **Running title:** range-wide multi-trait variation

5 **Keywords**: phenotypic variation, species distribution models, beech, acclimation, trait co-

6 variation, common gardens

7 **ABSTRACT**

8 **Aim:** To better understand and more realistically predict future species distribution ranges, it is

9 critical to account for local adaptation and phenotypic plasticity in populations' responses to

10 climate. This is challenging because local adaptation and phenotypic plasticity are trait-

11 dependent and traits co-vary along climatic gradients, with differential consequences for fitness.

12 Our aim is to quantify local adaptation and phenotypic plasticity of vertical and radial growth,

13 leaf flushing and survival across *Fagus sylvatica* range and to estimate each trait contribution to

14 explain the species occurrence**.**

15 **Location:** Europe

16 **Time period:** 1995 – 2014; 2070

17 **Major taxa studied:** *Fagus sylvatica L.*

18 **Methods:** We used vertical and radial growth, flushing phenology and mortality of *Fagus*

19 *sylvatica* L. recorded in BeechCOSTe52 (>150,000 trees). Firstly, we performed linear mixed-

20 effect models that related trait variation and co-variation to local adaptation (related to the

21 planted populations' climatic origin) and phenotypic plasticity (accounting for the climate of the

22 plantation), and we made spatial predictions under current and RCP 8.5 climates. Secondly, we

23 combined spatial trait predictions in a linear model to explain the occurrence of the species.

24 **Results:** The contribution of plasticity to intra-specific trait variation is always higher than that

25 of local adaptation, suggesting that the species is less sensitive to climate change than expected;

26 different traits constrain beech's distribution in different parts of its range: the northernmost edge

27 is mainly delimited by flushing phenology (mostly driven by photoperiod and temperature), the

28 southern edge by mortality (mainly driven by intolerance to drought), and the eastern edge is

29 characterised by decreasing radial growth (mainly shaped by precipitation-related variables in

30 our model); considering trait co-variation improved single-trait predictions.

31 **Main conclusions:** Population responses to climate across large geographical gradients are

32 dependent on trait x environment interactions, indicating that each trait responds differently

33 depending on the local environment.

34

35

36

37

38

39

40

41

42

43

44

45

46

1. INTRODUCTION

Climate change is having a major impact on the structure, composition and distribution of forests worldwide (Trumbore *et al.*, 2015). Accordingly, numerous models have projected significant range shifts of forest tree species towards higher latitudes and elevations (Urban *et al.*, 2016). However, to date, the two most important processes in the response of tree populations to a rapidly changing climate, local adaptation and phenotypic plasticity (Savolainen *et al.*, 2007; Aitken *et al.*, 2008), are not systematically considered by species distribution models (Valladares *et al.*, 2014; Duputié *et al.*, 2015; Richardson *et al.*, 2017). Phenotypic plasticity enables a given genotype to express different phenotypes in response to changing environments, while local adaptation produces new genotypes with a greater ability to cope with the new environment. The two mechanisms are ubiquitous in natural populations, although their respective importance is considered to vary extensively through time and across species ranges (Reich *et al.*, 2016; Des Roches *et al.*, 2018). To persist under rapid climatic change, organisms with short generation times can take advantage of evolutionary responses and phenotypic plasticity (Scheepens *et al.*, 2018), whereas organisms with long generation cycles will rely predominantely on phenotypic plasticity (Fox *et al.*, 2019). To better understand and more realistically predict future species distribution ranges, it is therefore critical to identify and quantify the respective importance of local adaptation and phenotypic plasticity in the response of local populations to a changing climate.

From an ecological perspective, fitness can be associated with several phenotypic traits which directly affect survival and reproduction, creating a fitness landscape (Laughlin, 2018) that allows them to be used to bound species ranges (Benito-Garzón *et al.*, 2013; Stahl *et al.*, 2014). From a biogeographical perspective, higher fitness can be associated with higher probabilities of occurrence of a species in a given environment (Jiménez *et al.*, 2019). Fitness-related traits vary

70   across large geographical gradients, mainly depending on how natural selection drove differences

71   among populations in the past. For instance, tree height is generally greatest at the core of a species

72   range and decreases towards its margins (Purves, 2009; Pedlar & McKenney, 2017). Climate-

73   driven mortality commonly increases towards the driest part of a species range, which is related to

74   drought-induced stress conditions (Benito Garzón *et al.*, 2018). The onset of flushing phenology

75   tends to be delayed towards high latitudes (Duputié *et al.*, 2015) as a consequence of genetic

76   adaptation to late frost and fluctuating photoperiod (Way & Montgomery, 2015). Moreover, traits

77   tend to co-vary across climatic gradients (Laughlin & Messier, 2015). A conspicuous example is

78   the demographic compensation found between survival and growth near range margins (Doak &

79   Morris, 2010; Benito-Garzón *et al.*, 2013; Peterson *et al.*, 2018), and further delimitation of species

80   ranges based on demographic approaches (Merow *et al.*, 2017). New climatic conditions can result

81   in maladaptation of some populations, which may change intra-specific patterns of trait variation

82   and co-variation across geographical gradients, and eventually, species ranges. For example,

83   increasing temperatures at high-latitude or high-elevation range margins are likely to produce

84   higher growth rates, but they can also induce higher mortality owing to late frosts (Vitasse *et al.*,

85   2014; Delpierre *et al.*, 2017). Hence, species ranges are likely to be delimited by the interaction of

86   multiple traits and their responses across environmental gradients (Benito-Garzón *et al.*, 2013;

87   Stahl *et al.*, 2014; Enquist *et al.*, 2015).

88   Common gardens or provenance tests provide us with the necessary experiments to

89   quantify phenotypic plasticity and local adaptation of fitness-related traits in response to climate

90   (Mátyás, 1999). Models based on reaction norms of phenotypic traits using measurements

91   recorded in common gardens show that: (i) geographic variation in populations' responses to

92   climate is more strongly based on phenotypic plasticity than on local adaptation (Benito Garzón *et*

93 *al.*, 2019); (ii) phenotypic variation can strongly differ among traits, in particular for survival of

94 young trees, growth, and flushing phenology - traits that are directly related to fitness and typically

95 measured in common gardens (Benito Garzón *et al.*, 2011; Valladares *et al.*, 2014; Duputié *et al.*,

96 2015; Richardson *et al.*, 2017); (iii) as a consequence, predictions of future species ranges are

97 likely to be strongly influenced by the combined response of different fitness-related traits to

98 climate (Laughlin, 2018), but this structured combination of intra-specific multi-trait variation

99 defining species ranges has not been explored with empirical data.

100 *Fagus sylvatica* L. (European beech, henceforth "beech") is a widely distributed deciduous

101 broadleaf temperate tree. In some parts of its range, beech has a late flushing strategy to avoid late

102 frosts, which has a generally detrimental effect on tree growth (Gömöry & Paule, 2011; Robson *et*

103 *al.*, 2013; Delpierre *et al.*, 2017). Beech is currently expanding at its northern distribution edge,

104 whereas it experiences drought-induced radial growth decline and increasing mortality at its

105 southern edge (Farahat & Linderholm, 2018; Stojnic *et al.*, 2018). The extent to which this pattern

106 will continue in the future depends on how the combination of several fitness-related traits will

107 influence the species' response to new climates.

108 Here, we propose a new modeling approach that quantifies local adaptation and phenotypic

109 plasticity of four major phenotypic traits related to fitness (vertical and radial growth, young tree

110 survival, and flushing phenology) and their interactions, to delimit species ranges under current

111 and future climates. The four traits studied are expected to be under natural selection and show

112 high heritability (Etterson, 2002; Delpierre *et al.*, 2017). Radial and vertical growth are directly

113 related with biomass and thus reproduction (Younginger *et al.*, 2017), and the timing of flushing

114 can affect fitness through reproduction success and growth by delimiting the growth season

115 (Chuine, 2010). We use the phenotypic measurements recorded in the BeechCOSTe52 database

116   (Robson *et al.*, 2018), the largest network of common gardens for forest trees in Europe, covering

117   virtually the entire distribution range of the species. Our specific objectives are: (i) to quantify

118   range-wide patterns of phenotypic plasticity and local adaptation in growth, young tree survival

119   and flushing phenology; (ii) to identify interactions among the different traits and the extent of

120   their geographical variation in local adaptation and phenotypic plasticity; (iii) to discuss how these

121   fitness-related traits delimit species ranges, and (iv) to better understand species ranges under new

122   climate scenarios and the role of trait variation in shaping the future species range.

123

124   **2. MATERIAL AND METHODS**

125   We calibrated two types of linear mixed-effect models using a combination of trait measurements

126   from common gardens where seeds coming from provenances from different origins have been

127   planted (provenances) and of environmental variables that we obtained for these common gardens

128   and provenances. The first model type (one-trait models) used single traits as response variables

129   and environmental data as explanatory variables. The second model type (two-trait models) added

130   a second trait as co-variate, which allowed the interaction of both traits to be accounted for in the

131   model. Finally, to quantitatively estimate the contribution of each trait to explain beech range, we

132   performed a binomial model using the occurrence of the species as response variable

133   (presence/absence) and the spatial predictions of all traits as explanatory variables.

134

135   **2.1. Trait measurements**

136   We analyzed total tree height (vertical growth), diameter at breast height (DBH; radial growth),

137   young tree survival and flushing phenology measured on a total of 153,711 individual beech trees

138   that originated from seeds collected from 205 populations (hereafter referred to as "provenances")

139   across Europe and planted at 38 common gardens (hereafter "trials") (Figure 1). Briefly, the seeds

140   were germinated in greenhouses and planted in the trials at an age of two years. Plantations were

141   carried out in two consecutive campaigns, the first campaign (comprising 14 trials) in 1995 and

142   the second one (comprising 24 trials) in 1998 (Robson *et al.*, 2018). This experimental design

143   allowed us to attribute the effect of the climate at the trials to phenotypic plasticity and the effect

144   of the climate at the provenance origin to genetics, including both the genetic structure and

145   adaptive potential of the provenances. Young tree survival was recorded as individual tree survival.

146   Leaf flushing was transformed from observational-stage score data (qualitative measurements that

147   slightly differ among trials) to Julian days by adjusting flushing stages for each tree in every trial

148   using the Weibull function (Robson *et al.*, 2011, 2013).

149

2.2. Environmental data

151   We used the EuMedClim database that gathers climatic information from 1901 to 2014 gridded at

152   1km (Fréjaville & Benito Garzón, 2018). The climate of the provenances was averaged for the

153   period from 1901 to 1990, with the rationale that the seeds planted in the common gardens

154   stemmed from trees growing during that period (Leites *et al.*, 2012). To characterize the climate

155   of the common gardens, we calculated average values for the period between the date of planting

156   (either 1995 or 1998) and the year of measurement of each trait for 21 climate variables

157   (Supporting Information Table S1.2, Appendix S1).In addition, we used the latitude and longitude

158   of the provenance and of the trial as proxies for the photoperiod and continentality, respectively

159   (used in our flushing phenology models).

160   Phenotypic predictions under future climates were performed using the representative

161   concentration   pathway   (RCP   8.5)   in   GISS-E2-R   from   WorldClim

162   (http://www.worldclim.org/cmip5_30s) for 2070. We deliberately chose only this pessimistic

163   scenario because for long-lived organisms such as forest trees it makes little difference whether

164   the projected situation will be reached in 2070 or some decades later.

165

2.3. Statistical analysis

167   2.3.1. Spatial autocorrelation analysis

168   We performed a Moran's I analysis to check for spatial autocorrelation of vertical and radial

169   growth, young tree survival, and leaf flushing. Correlograms were used to check autocorrelation

170   variation with distance. We used the Moran.I function of the 'ape' package (Paradis *et al.*, 2018)

171   and the 'Correlog' function of the 'pgirmess' package (Giraudoux *et al.*, 2018).

172   2.3.2. Environmental variable selection

173   To avoid co-linearity and reduce the number of environmental variables to use in models, we

174   performed two principal component analyses (PCA), one for the climate variables related to the

175   provenance site and one for the climate variables related to the trial site. For tree height, DBH and

176   young tree survival, we considered 21 variables for the provenance and 21 variables for the trial

177   (Supporting Information Figure S1.3, Appendix S1); whereas for leaf flushing, we only included

178   the temperature-related variables as well as latitude and longitude (a total of 20 variables), because

179   leaf flushing is known to be mainly driven by them (Basler & Körner, 2014).

180   The retained variables after the PCA screening were combined in models containing one

181   variable to characterize the climate of the provenance and one variable to characterize the climate

182   of the trial (Supporting Information Table S1.3, Appendix S1).

183

184

185   2.3.3. One-trait and two-trait mixed-effect models

186   We used linear mixed-effect models to analyze the response of individual traits (one-trait models)

187   and the co-variation between two traits (two-trait models) to climate. We included the climate at

188   the provenance and the trial site as previously selected (Supplementary Table 1), the age of trees,

189   and for the leaf flushing model also latitude and longitude as fixed effects. The trial, blocks nested

190   within the trial and trees nested within block and trial, were included as random effects to control

191   for differences among sites and for repeated measurements of the same trees. The random effect

192   of the provenance was also included in the model. The common form of the one-trait model was:

193
$$log(TR_{ijk}) = \alpha_0 + \alpha_1(Age_{ik}) + \alpha_2(CP_{ij}) + \alpha_3(CT_{ik}) + \alpha_4(CP_{ij}^2) + \alpha_5(CT_{ik}^2) + \alpha_6(Age_{ik} \times CP_{ij}) + \alpha_7(Age_{ik} \times CT_{ik}) + \alpha_8(CP_{ij} \times CT_{ik}) + \beta + \varepsilon$$

194   (Equation 1)

195   Where TR = trait response of the ith individual of the jth provenance in the kth trial; Age = tree age

196   of the ith individual in the kth trial; CP = climate at the provenance site of the ith individual of the

197   j^{th} provenance; CT = climate at the trial site of the ith individual in the kth trial; β = random effects

198   and ε = residuals. In addition, the model included the following interaction terms: Age and CP,

199   Age and CT, and CP and CT.

200   We analyzed trait co-variation across the species range by adding two specific traits of

201   interest in the same model. The common form of the two-trait model was:

202    $$log(TR_{ijk}) = \alpha_0 + \alpha_1(Age_{ik}) + \alpha_2(Cov_{ij}) + \alpha_3(CP_{ij}) + \alpha_4(CT_{ik}) + \alpha_5(Cov_{ik} \times CP_{ij}) + \alpha_6$$

203    $$(Cov_{ik} \times CT_{ik}) + \alpha_7(Cov_{ik} \times Age_{ik}) + \alpha_8(Age_{ik} \times CP_{ij}) + \alpha_9(Age_{ik} \times CT_{ik}) + \alpha_{10}(CP_{ij} \times CT_{ik})$$
204    $$+ \beta + \varepsilon$$

205   (Equation 2)

206   Where TR = trait response of the ith individual of the jth provenance in the kth trial; Age = tree age

207   of the ith individual in the kth trial; Cov = trait co-variate of the ith individual in the kth trial; CP =

208   climate at the provenance site of the ith individual of the jth provenance; CT = climate at the trial

209   site of the ith individual in the kth trial; β = random effects and ε = residuals. In addition, the model

210   included the following interaction terms: Cov and CP, Cov and CT, Cov and Age, Age and CP,

211   Age and CT, and CP and CT.

212   The one-trait and two-trait models for vertical and radial growth and leaf flushing were

213   fitted with the 'lmer' function, while the one-trait model for young tree survival was fitted with

214   the 'glmer' function to accommodate logistic regressions (binomial family) in the analysis. We

215   implemented a stepwise-model procedure with four main steps to choose the best supported model

216   (Akaike, 1992): (i) we fitted saturated models that included all the variables in the fixed part of the

217   model; (ii) we chose the optimal random component of the model by comparing the battery of

218   models using restricted maximum likelihood (REML), and selected the best model using the

219   Akaike information criterion (AIC) with criteria ΔAIC <2 (Mazerolle, 2006); (iii) we compared

220   the battery of models using maximum likelihood (ML) and selected the optimal fixed component

221   using the AIC criterion; (iv) we combined the best optimal random and fixed component

222   previously selected and adjusted them using REML to obtain the best performing model. All model

223   fits were done using the package 'lme4' (Bates *et al.*, 2018).

224   For the best supported models, we visually analyzed the interactions of vertical growth,

225   radial growth, young tree survival and leaf flushing with the environment (one-trait models) and

226   between traits (between the response and co-variate variable, i.e. the two-trait models). To do so,

227   tree age was fixed to 12 years for the radial and vertical growth and leaf flushing models and to 6

228   years for the young tree survival model. Mathematical interactions in one-trait models (CP x CT

229   in equation 1) represent the differences in trait values that can be attributed to the provenance

230   (interpretable as local adaptation) and those that can be attributed to the trial (interpretable as

231   phenotypic plasticity). Mathematical interactions in two-trait models (Cov x CT in equation 2)

232   represent the differences in trait values that can be attributed to a second trait that co-varies across

233   the species range with the first trait, mediated by the climate of the trial (representing phenotypic

234   plasticity). Unfortunately, young tree survival could not be included in the two-trait models

235   because there were insufficient measurements shared with other traits in the same trials.

236   We estimated the percentage of the variance explained by the model attributed to the fixed

237   effects alone (marginal R^2) and attributed to the fixed and random effects together (conditional

238   R^2). We measured the generalization capacity (Pearson correlation) of the model using cross-

239   validation (64% of the data used for calibration and the remaining 34% for validation).

240   2.3.4. Spatial predictions

241   We made spatial predictions for each trait across the species range for current and future climatic

242   conditions using the 'raster' package (Hijmans *et al.*, 2017). For the prediction of current and

243   future trait variation, the climate variable for provenance was represented by the average climate

244   over the period from 1901 to 1990. The climate of the trial was set as the average climate from

245   2000 to 2014, for current trait predictions, and to 2070 for future predictions. For two-trait models,

246   the predicted values of the co-variate (DBH and leaf flushing) in the present were used to estimate

247   the predictions of vertical growth in the future. We calculated the spatial difference between the

248   future and the current conditions (future values minus current values) to illustrate the amount of

249   change that traits can accommodate. All spatial predictions of traits were delimited within the

250   distribution range of the species (EUFORGEN, 2009).

251   2.3.5. Quantification of the trait contribution to delimit the range of beech

252   Following the rationale that fitness-related, demographic and functional traits can shape species

253   ranges (Stahl *et al.*, 2014; Merow *et al.*, 2017), we regressed the occurrence (presence/absence) of

254   the species (EUFORGEN, 2009) against the trait values obtained by the one-trait models using the

255   'glm' function to accommodate logistic regressions (binomial family). The equation takes the

256   form:

257    $$(RV) = \alpha_0 + \alpha_1(Vg) + \alpha_2(Rg) + \alpha_3(S) + \alpha_4(Lf) + \alpha_5(Vg \times S) + \alpha_6(Rg \times S) + \alpha_7(Lf \times S) + \alpha_8(Vg \times Rg) + \alpha_9(Vg \times Lf) + \alpha_{10}(Rg \times Lf) + \varepsilon$$

258   (Equation 3)

259   Where RV = presence/absence of beech; Vg = vertical growth; Rg = radial growth; S = young tree

260   survival; Lf = leaf flushing; ε = residuals. In addition, the model included all possible pairwise

261   linear interactions of the included traits. The total deviance explained by the model was calculated

262   using the function 'Dsquared' of the package 'modEvA' (Barbosa *et al.*, 2014). Then, we

263   performed an analysis of variance (ANOVA) of the model to obtain trait and trait interaction

264   deviances to estimate the percentage of the variance attributable to each trait.

265 All the models where performed with the R statistical framework version 3.2.0 (R Development

266 Core Team, 2015).

267

268 **3. RESULTS**

269 **3.1. Spatial autocorrelation analysis**

270 Overall, the four studied traits were not significantly autocorrelated (Supporting Information Table

271 S1.1, Appendix S1), although one autocorrelation point was found for young tree survival and leaf

272 flushing using distance correlograms (Supporting Information Figure S1.1, Appendix S1).

273

274 **3.2. Environmental variables selection**

275 The two PCA performed (provenance PCA and trial PCA) revealed two groups of variables, one

276 related with temperature and another more related with precipitation (Supporting Information

277 Figure S1.2, Appendix S1). The two most important axes of the provenance PCA explained 53.52

278 and 24.03% of the total variance, and those of the trial PCA explained 38.93 and 24.19%

279 (Supporting Information Figure S1.2, Appendix S1). To avoid co-linearity in the variables that we

280 used in the model stepwise procedure, we retained the following variables for tree growth and

281 young tree survival: BIO1, BIO5, BIO6, BIO12, BIO13, BIO14, PET Mean and PET Max. For

282 the leaf flushing models, we retained BIO1, BIO5, BIO6, MTdjf, MTmam, MTjja, Mtson, and

283 Mtdjfmam in addition to latitude and longitude.

284

285 **3.3. One-trait and two-trait models**

286   According to the best supported models (Table 1 and Supporting Information Table S1.3,

287   Appendix S1), the most important variable related to the climate at the provenance for vertical

288   growth, radial growth and young tree survival was maximal potential evapotranspiration (PET

289   Max). The most important variables related to climate at the trials were precipitation of the wettest

290   month (BIO13) for vertical growth, annual precipitation (BIO12) for radial growth, and

291   precipitation of the driest month (BIO14) for young tree survival. In the case of leaf flushing, the

292   mean temperature of December, January and February (MTdjf) was the most important climate

293   variable for both the provenance and the trial site. The latitude of the provenance and the trial and

294   the longitude of the trial were also significant in the leaf flushing model (see Supporting

295   Information Table S1.3, Table S1.4, Appendix S1 for detailed statistics on the models). We

296   observed significant interactions between the climate of the trial and that of the provenance in all

297   models (Table 1; Supporting Information Table S1.4, Appendix S1).

298   The capacity for generalization from the models (Pearson correlation coefficients) was high:

299   between 0.53 for radial growth and 0.73 for leaf flushing. The marginal R^2 ranged from 18% for

300   the young tree survival model to 57% for the vertical growth model, while the conditional R^2

301   ranged from 40% for the young tree survival model to 98% for the radial growth model (Supporting

302   Information Table S1.4, Appendix S1).

303   The significance of the fixed and random effects in the one-trait models was positively

304   affected (i.e., estimates were higher) by the addition of a second trait (Supporting Information

305   Table S1.5, Appendix S1). Furthermore, the co-variates and their interactions with the climate

306   variables of the trials were also significant in the two-trait models (Supporting Information Table

307   S1.5, Appendix S1). The capacity to generalize from the two-trait models was high: 0.76 for the

308   vertical growth-radial growth model and 0.77 for the vertical growth-leaf flushing model

309   (Supporting Information Table S1.5, Appendix S1). The marginal R^2 was 62% in the vertical

310   growth-radial growth model and 47% in the vertical growth-leaf flushing model, while the

311   conditional R^2 was 95% in the vertical growth-radial growth model and 99% in the vertical growth-

312   leaf flushing model (Supporting Information Table S1.5, Appendix S1).

313

3.4. Spatial patterns of phenotypic trait variation from one-trait models

315   Spatial predictions showed differences in phenotypic trait variation among traits (Figure 2, maps)

316   and the interaction graphs permitted the way that plasticity and local adaptation shape these

317   differences to be visualized (Figure 2, interaction graphs).

318   Vertical growth reached its maximum value at intermediate values of precipitation of the

319   wettest month in the trials (Figure 2a, interaction graph). These largest trees were predicted to

320   occur mostly over the northern and western part of the species range (Figure 2a, map). A signal of

321   local adaptation to PET max was detected in our models and is shown by the interaction graph,

322   where each line represents the response of provenances to high, intermediate and low levels of

323   maximal potential evapotranspiration.

324   Predicted radial growth across the species range presented a similar pattern to that of

325   vertical growth, but with the lowest values in marginal populations, particularly at the southern

326   margin (Figure 21b, map). High annual precipitation coincided with high growth rates (Figure 2b

327   map), with a moderate signal of local adaptation to PET max in the form of some variation among

328   provenances (Figure 2b, interaction graph).

329   The lowest young tree survival rates were predicted towards the east and at some isolated

330   points in the southernmost part of the range (Figure 2c, map). Young tree survival increased

331 towards those trials where precipitation is high in the driest month, with weak local adaptation to

332 PET max indicated by very small –though statistically significant– differences among provenances

333 (Figure 2c, interaction graph).

334   Earlier flushing was predicted towards the south-eastern part of the range (Fig 1d, map),

335 with notable local adaptation indicated by large differences among provenances depending on the

336 latitude of origin (Figure 2d, interaction graph). Differences in flushing date among provenances

337 were particularly large in trials where the winter temperature is low (Figure 2d, interaction graph).

338

339 **3.5. Patterns of phenotypic trait variation from two-trait models**

340 Overall, models with a second trait as co-variate produced different results to those considering a

341 single trait only. Predicted vertical growth was higher when either radial growth (Figure 3a) or leaf

342 flushing (Figure 3b) was included as a co-variate than when no co-variates were considered (Figure

343 2a). Vertical growth increased with radial growth and precipitation (Figure 3a) and decreased in

344 those regions where leaf flushing was predicted to be late in the year (which corresponded mainly

345 to the northern part of the range) (Figure 3b).

346

347 **3.6. Spatial predictions of traits under climate change considering one- and two-trait models**

348 Trait projections for 2070 showed an overall increase in tree growth, particularly for radial growth

349 (Figure 4a, b), but following similar spatial patterns to those predicted under current conditions

350 (Figure 2a, b). Young tree survival was predicted to strongly decrease (with respect to that

351 predicted under current conditions, Figure 2c) in the east and throughout the range periphery, while

352   young tree survival rates remained higher in the central part (Figure 4c). Leaf flushing showed

353   similar patterns to those predicted under current conditions (Figure 2d) but with an overall advance

354   in flushing dates (Figure 4d).

355   The prediction of vertical growth, considering radial growth as a covariate, showed an

356   overall increase across the distribution range (Figure 4e) with respect to the model projection of

357   vertical growth without radial growth as a covariate under future conditions (Figure 4a).

358   Nevertheless, the predictions of vertical growth considering radial growth as a covariate (Figure

359   4e) showed an overall decrease in vertical growth, with some increases in vertical growth in the

360   northern and northeastern range, compared to the same model applied to current conditions (Figure

361   3a; Supporting Information Figure S1.3e, Appendix S1). Predictions considering leaf flushing as

362   a co-variate tended to constrain vertical growth throughout the range (Figure 4f) compared with

363   the same model in current conditions (Figure 3b).

364

3.7. Total trait contribution to explain species ranges

366   All traits and their interactions significantly contributed to explain species occurrence (Table 2).

367   The model explained 31% of the total deviance, with vertical growth accounting for 37%, radial

368   growth for 33%, young tree survival for 19%, and leaf flushing for 1%. Please note that the

369   different contribution of these four traits explaining species occurrence may be constrained by the

370   nature of the data (particularly survival that is only measured in young trees). The interaction

371   between vertical growth and young tree survival contributed with 3% to the total deviance, that

372   between radial growth and leaf flushing with 2% and the remaining interactions with 1% or less

373   (Table 2).

374

4. DISCUSSION

376

4.1. Contribution of phenotypic plasticity and local adaptation to range-wide variation in beech growth, young tree survival and leaf flushing

379 Altogether, our results underpin that range-wide variation in fitness-related traits of beech is driven

380 markedly more by phenotypic plasticity than by local adaptation (Supporting Information Table

381 S1.4, Appendix S1), as happens in other plant species (Benito Garzón *et al.*, 2019), and they imply

382 that beech possesses a noteworthy capacity to respond to rapid climate change through

383 acclimation. Although a short-term response through acclimation can be considered as positive for

384 beech to keep pace with climate change, our results point out that the plastic component of tree

385 growth and young tree survival is mostly related to precipitation (Table 1), which follows highly

386 unpredictable patterns (Pflug *et al.*, 2018), making it difficult to evaluate whether acclimation will

387 be enough for beeches to survive (our predictions for 2070 under RCP 8.5. showing an increase of

388 mortality in young trees at the margins of the species ranges suggest that acclimation will not be

389 great enough to permit the species to survive, at least at the margins of its range – Figure 4c). Local

390 adaptation in tree growth (vertical and radial) and young tree survival are driven by adaptation to

391 maximal potential evapotranspiration (Table 1), suggesting that populations are responding to

392 selection factors related to drought (Volaire, 2018). This is in agreement with the general

393 consensus that beech is a drought-sensitive species (Aranda *et al.*, 2015), although there is ongoing

394 debate over the extent of resistance that beech has to drought (Pflug *et al.*, 2018).

395   The plastic response of leaf flushing to climate was mainly driven by winter temperatures

396   (Table 1). There is a general consensus that winter temperatures will increase globally in the future

397   (Vautard *et al.*, 2014), and, accordingly, our projection for 2070 anticipates an advance in flushing

398   through most of the range (Figure 2d, 3d and S3d). However, leaf flushing can be constrained by

399   local adaptation to photoperiod (Way & Montgomery, 2015; Gauzere *et al.*, 2017). The fact that

400   phenotypic plasticity and local adaptation in leaf flushing are driven by different environmental

401   parameters implies that these two processes would interact in the long-term. For instance,

402   phenotypic plasticity concerning winter temperatures might enhance local adaptation towards new

403   photoperiodical cues (i.e., shorter spring days), but the evolutionary time scale of local adaptation

404   makes this interaction very unlikely in the short-term.

405

406   4.2 Trait relationships across the species range

407   Trait inter-dependence varied along geographical gradients as the two-trait models had higher

408   predictive power and explained more variance than those based on a single trait (Supporting

409   Information Table S1.4 and S1.5, Appendix S1). The tight albeit not perfect positive interaction

410   between tree vertical and radial growth (Figure 3a, interaction graph) is unsurprising because of

411   allometric relationships between these two variables, particularly in a common-garden plantation

412   that avoids competition among trees.

413   The biological basis of the observed co-variation between vertical growth and leaf flushing

414   is less obvious. One possible explanation is that vertical growth is greatly restricted by late flushing

415   in northern beech populations (Kollas *et al.*, 2014). This would also explain our observation that

416   the one-trait model predicts taller trees to occur in the North, whereas the two-trait model predicts

417   just the opposite. Interestingly, the two-trait model thus implies that strong local adaptation of leaf

418   flushing to photoperiod tends to constrain phenotypic plasticity for vertical growth in northern

419   beech populations (Way & Montgomery, 2015).

420

4.3. Are spatial patterns of growth, young tree survival and leaf flushing delimiting the range of beech?

421

422

423   Beech populations from certain eastern and southern parts of the distribution range seem most

424   sensitive to climate, as suggested by the lowest values for all traits considered (Figure 2). In other

425   parts of beech's range, different traits respond differently to climate, in line with the patterns found

426   in annual plants and wood scrubs (Merow *et al.*, 2017). Our analysis of species occurrence as a

427   function of spatial trait values also suggests that each of these traits and their interactions

428   contributed to some extent to the delimitation of the species range (31% of the variance is

429   explained by the four traits; Table 3). In particular: (i) young tree mortality delimits certain parts

430   of the southern and eastern range of beech, reflecting the marginality due to climate continentality

431   in these areas, and meaning that these populations are most threatened, thus making eastwards

432   expansion of beech difficult (survival was exclusively measured in young trees, reflecting

433   recruitment processes that are largely limited to climatically favorable years, indicating that more

434   studies on regeneration and mortality are needed to confirm this result); this is the case for many

435   species whose highest mortality is in the driest part of their range (Benito-Garzón *et al.*, 2013;

436   Anderegg *et al.*, 2015; Camarero *et al.*, 2015); (ii) the smallest girths are predicted in the southern

437   part of the distribution and the eastern part of the range, suggesting that radial growth is mostly

438   restricted by drought (interaction graph and map, Figure 2b), as has already been pointed out

439   (Farahat & Linderholm, 2018); (iii) with very little variation across climatic gradients, vertical

440 growth alone will not delimit beech range. This is not the case for other tree species, for which tree

441 height is clearly delimiting species range (Chakraborty *et al.*, 2018), highlighting the fact that no

442 single best trait delimits tree species ranges; (iv) projections of trees growing in southern and

443 south-eastern regions that flush early also have higher mortality and lower growth predictions than

444 elsewhere within the species range. However, when tree height and leaf flushing are pooled

445 together in the two-trait model, this leads to an decrease in vertical growth in the North; (v) it

446 seems that in beech, and likely in other species with local adaptation to photoperiod, phenology

447 could restrict the northern expansion of ranges (Duputié *et al.*, 2015; Saltré *et al.*, 2015). Although

448 the link between phenology, young tree survival and fitness is still unclear, and more experiments

449 would provide a better understanding the interaction between photoperiod and phenology.

450

4.4. Implications of using trait approaches based on phenotypic variation to forecast beech
451

452 **sensitivity to climate change**

453 Overall, spatial patterns of vertical and radial growth, young tree survival and leaf flushing

454 predicted for the future (Figure 4), are relatively similar to those predicted by the models under

455 current conditions (Figure 2 & 3). This might be due to the high plasticity of these traits that allows

456 populations to respond to short-term changes in their environment, but other factors such as

457 dispersal capacity, geographical or human barriers, and adjustment of climatic scenarios for the

458 future would change our predictions. Our results, based on the study of phenotypic variation,

459 predict species persistence in the future (if the occurrence of the species can be linked to high trait

460 values (Merow *et al.*, 2017)) rather than extinction and migration northwards as predicted by

461 species distribution models based on the occurrence of the species (Kramer *et al.*, 2010; Stojnic *et*

462 *al.*, 2018).

463   Nevertheless, the direct comparison of our trait predictions for current and future

464   conditions allows us to detect some differences in their spatial patterns and total trait values

465   (Supporting Information Figure S1.3, Appendix S1), and gives us a better understanding of the

466   temporal dynamics of traits and their relative importance for beech persistence in the future. For

467   instance, our models of leaf flushing predict reduced geographical variability in phenology in the

468   future (from day 94 to 160 -Figure 2d- and from day 94 to 147 – Figure 4d-), as has been reported

469   worldwide (Ma *et al.*, 2018). This is mostly explained by larger advances in the phenology of

470   populations at colder sites than those at warmer sites, likely as a consequence of the larger

471   increases in winter temperatures that happen in the North (Kjellström *et al.*, 2018). Survival of

472   young trees is predicted to decrease at the margins of the distribution, but less markedly than is

473   predicted by species distribution models (Kramer *et al.*, 2010; Stojnic *et al.*, 2018). Although our

474   spatial trait predictions do not perfectly match species occurrence, they explain the adaptive and

475   plastic responses of populations' fitness-related traits to climate (Benito Garzón *et al.*, 2019).

476   Including more than one trait related to growth likely reflects a conserved allometric

477   relationship between vertical and radial growth in the future (Figure 4e), but this may be a direct

478   consequence of the lack of competition among trees in our experimental design. Including

479   phenology in two-trait models seems to be detrimental for vertical growth, at least for northern

480   populations where growth is likely constrained by phenology (Figure 4f). However, our trait co-

481   variation approaches are limited to vertical growth as response variables, limiting our

482   understanding of the interplay that other traits can have across species range in the future.

483

484   **4.5. Limitations, perspectives and future research**

485   Although this study relied on the largest network of common gardens for a forest tree in Europe,

486   the resulting inferences suffer from a number of limitations. Our models are based on a limited set

487   of ages (from 2 to 15 years old). However, the expression of phenotypic plasticity changes with

488   age (Mitchell & Bakker, 2014), which can restrict the broad scope of our results to those ages that

489   we considered. This limitation is particularly pronounced for the case of survival (age range 2 to

490   6 years), for which data only reflect early recruit survival. Our models of young tree mortality can

491   also reflect the quality of the data from common gardens, where recruit survival was measured

492   over a short study period and did not necessarily faithfully capture the regeneration potential of

493   forest tree populations.

494   Tree growth and phenology are directly related to fitness (Chuine, 2010; Delpierre *et al.*,

495   2017; Younginger *et al.*, 2017). However, other relevant proxies for tree fitness as fecundity and

496   reproduction have not been considered in our approach. In beech, climate warming tends to

497   increase seed production in northern populations (Drobyshev *et al.*, 2010) and to cause a decline

498   in seedling density in southern ones (Barbeta *et al.*, 2011), which would be expected to continue

499   under climate change.

500   Our approach reflects the plastic and adaptive components of traits to determine their

501   spatial distribution. Important elements of spatial ecology, such as geographical barriers and trees'

502   dispersal capacity (Svenning & Skov, 2005), competition and other biotic interactions across large

503   geographical gradients (Archambeau *et al.*, 2019) and those aspects related with the uncertainty of

504   future climate (Nazarenko *et al.*, 2015), are not considered in our approach. . Adding these

505   processes to our models would open a new perspective, to extend understanding of the realized

506   niche of the species ranges. The genetic effect attributed to the provenances in our models includes

507   both the genetic structure and the potential of populations to adapt. As more genomic information

508   on adaptive traits becomes available, models could incorporate the genomic basis of climate

509   adaptation to help separate these different genetic effects (Bay *et al.*, 2018)

510   Our predictions should help to shape future controlled experiments on those populations

511   most sensitive to climate (in the South – East of the range), and others designed to test those trait

512   relationships that are still unclear (phenology – growth – mortality) at the northernmost distribution

513   edge. Although both for beech, and for tree species in general, plasticity is thought to help

514   populations to persist under climate change (Benito Garzon et al. 2019), evolutionary processes

515   can play an crucial role for annual plants and those organisms with short generation cycles,

516   permitting them to adapt to new climate conditions (Scheepens *et al.*, 2018; Fox *et al.*, 2019). Both

517   theoretical and empirical studies on the interplay between phenotypic plasticity and local

518   adaptation across organisms with different life-history strategies are needed to fully understand

519   how these two processes modify populations' responses to climate change.

520

521

522   **REFERENCES**

523   Aitken, S.N., Yeaman, S., Holliday, J.A., Wang, T. & Curtis-Mclane, S. (2008) Adaptation , migration or

524   extirpation : climate change outcomes for tree populations. *Evolutionary Applications*, 95–111.

525   Akaike, H. (1992) Data analysis by statistical models. *No To Hattatsu*, **24**, 127–133.

526   Anderegg, W.R.L., Flint, A., Huang, C., Flint, L., Berry, J.A., Davis, F.W., Sperry, J.S. & Field, C.B.

527   (2015) Tree mortality predicted from drought-induced vascular damage. *Nature Geoscience*, **8**, 367–

528   371.

529   Aranda, I., Cano, F.J., Gascó, A., Cochard, H., Nardini, A., Mancha, J.A., López, R. & Sánchez-Gómez,

530   D. (2015) Variation in photosynthetic performance and hydraulic architecture across European

531   beech Fagus sylvatica L .) populations supports the case for local adaptation to water stress. *Tree*

532   *Physiology*, **35**, 34–46.

533   Archambeau, J., Ruiz-Benito, P., Ratcliffe, S., Fréjaville, T., Changenet, A., Munoz Castaneda J.,

534   Lehtonen, A., Dahlgren, J., Zavala, M.A. & Benito Garzón, M. (2019) Similar patterns of

535   background mortality across Europe are mostly driven by drought in European beech and a

536   combination of drought and competition in Scots pine.

537   https://www.biorxiv.org/content/10.1101/551820v1

538   Barbeta, A., Peñuelas, J., Ogaya, R. & Jump, A.S. (2011) Reduced tree health and seedling production in

539   fragmented Fagus sylvatica forest patches in the Montseny Mountains (NE Spain). *Forest Ecology*

540   *and Management*, **261**, 2029–2037.

541   Barbosa, A.M., Brown, J.A. & Real, R. (2014) modEvA – an R package for model evaluation and

542   analysis. R package, version 0.1. Available at: http://modeva.r-forge.r-project.org/.

543   Basler, D. & Körner, C. (2014) Photoperiod and temperature responses of bud swelling and bud burst in

544   four temperate forest tree species. *Tree Physiology*, **34**, 377–388.

545   Bates, D., Maechler, M., Bolker, B., Walker, S., Bojesen, R.H., Singmann, H., Dai, B., Scheipl, F.,

546   Grothendieck, G. & Green, P. (2018) lme4: Linear mixed-effects models using Eigen and S4. R

547   package version 1.1-18-1. Available at: http://CRAN.R-project. org/package=lme4. *Available at:*

548   *http://CRAN.R-project. org/package=lme4*.

549   Bay, R.A., Harrigan, R.J., Underwood, V. Le, Gibbs, H.L., Smith, T.B. & Ruegg, K. (2018) Genomic

550   signals of selection predict climate-driven population declines in a migratory bird. *Science*, **359**, 83–

551   86.

552   Benito-Garzón, M., Ruiz-Benito, P. & Zavala, M.A. (2013) Interspecific differences in tree growth and

553   mortality responses to environmental drivers determine potential species distributional limits in

554   Iberian forests. *Global Ecology and Biogeography*, **22**, 1141–1151.

555   Benito Garzón, M., Alía, R., Robson, T.M. & Zavala, M.A. (2011) Intra-specific variability and plasticity

556   influence potential tree species distributions under climate change. *Global Ecology and*

557   *Biogeography*, **20**, 766–778.

558   Benito Garzón, M., Gonzalez Munoz, N., Wigneron, J.-P., Moisy, C., Fernandez-Manjarres, J. & Delzon,

559   S. (2018) The legacy of water deficit on populations having experienced negative hydraulic safety

560   margin. *Global Ecology & Biogeography*, **27**, 346–356.

561   Benito Garzón, M., Robson, T.M. & Hampe, A. (2019) ΔTraitSDM: species distribution models that

562   account for local adaptation and phenotypic plasticity. *New Phytologist*.

563   https://nph.onlinelibrary.wiley.com/doi/full/10.1111/nph.15716

564   Camarero, J.J., Gazol, A., Sancho-Benages, S. & Sangüesa-Barreda, G. (2015) Know your limits?

565   Climate extremes impact the range of Scots pine in unexpected places. *Annals of Botany*, **116**, 917–

566   927.

567   Chakraborty, D., Schueler, S., Lexer, M.J. & Wang, T. (2018) Genetic trials improve the transfer of

568   Douglas-fir distribution models across continents. *Ecography*, **41**, 1–14.

569   Chuine, I. (2010) Why does phenology drive species distribution? *Philosophical Transactions of The*

570   *Royal Society B Biological Sciences*, **365**, 3149–3160.

571   Delpierre, N., Guillemot, J., Dufrêne, E., Cecchini, S. & Nicolas, M. (2017) Tree phenological ranks

572   repeat from year to year and correlate with growth in temperate deciduous forests. *Agricultural and*

573   *Forest Meteorology*, **234**–**235**, 1–10.

574   Doak, D.F. & Morris, W.F. (2010) Demographic compensation and tipping points in climate-induced

575   range shifts. *Nature*, **467**, 959–962.

576   Drobyshev, I., Övergaard, R., Saygin, I., Niklasson, M., Hickler, T., Karlsson, M. & Sykes, M.T. (2010)

577   Masting behaviour and dendrochronology of European beech (Fagus sylvatica L.) in southern

578   Sweden. *Forest Ecology and Management*, **259**, 2160–2171.

579 Duputié, A., Rutschmann, A., Ronce, O. & Chuine, I. (2015) Phenological plasticity will not help all

580   species adapt to climate change. *Global Change Biology*, **21**, 3062–3073.

581 Enquist, B.J., Norberg, J., Bonser, S.P., Violle, C., Webb, C.T., Henderson, A., Sloat, L.L. & Savage,

582   V.M. (2015) Scaling from Traits to Ecosystems: Developing a General Trait Driver Theory via

583   Integrating Trait-Based and Metabolic Scaling Theories. *Advances in Ecological Research*, **52**, 249–

584   318.

585 Etterson, J.R. (2002) Constraint to Adaptive Evolution in Response to Global Warming. *Science*, **294**,

586   151–154.

587 EUFORGEN (2009) Distribution map of Beech (Fagus sylvatica). Available at: www.euforgen.org.

588   *www.euforgen.org*, 1.

589 Farahat, E. & Linderholm, H.W. (2018) Growth–climate relationship of European beech at its northern

590   distribution limit. *European Journal of Forest Research*, **137**, 1–11.

591 Fox, R.J., Donelson, J.M., Schunter, C., Ravasi, T. & Gaitán-Espitia, J.D. (2019) Beyond buying time: the

592   role of plasticity in phenotypic adaptation to rapid environmental change. *Philosophical*

593   *Transactions of the Royal Society B: Biological Sciences*, **374**, 20180174.

594 Fréjaville, T. & Benito Garzón, M. (2018) The EuMedClim Database: Yearly Climate Data (1901 – 2014)

595   of 1 km Resolution Grids for Europe and the Mediterranean Basin. *Frontiers in Ecology and*

596   *Evolution*, **6**, 1–5.

597 Gauzere, J., Delzon, S., Davi, H., Bonhomme, M., Garcia de Cortazar-Atauri, I. & Chuine, I. (2017)

598   Integrating interactive effects of chilling and photoperiod in phenological process-based models. A

599   case study with two European tree species: Fagus sylvatica and Quercus petraea. *Agricultural and*

600   *Forest Meteorology*, **244**–**245**, 9–20.

601 Giraudoux, P., Antonietti, J.-P., Beale, C., Pleydell, D. & Treglia, M. (2018) Package 'pgirmess'.

602   Available at: https://cran.r-project.org/web/packages/pgirmess/pgirmess.pdf.

603   Gömöry, D. & Paule, L. (2011) Trade-off between height growth and spring flushing in common beech

604   (*Fagus sylvatica* L.). *Annals of Forest Science*, **68**, 975–984.

605   Hijmans, R.J., Van Etten, J., Cheng, J., Mattiuzzi, M., Sumner, M., Greenberg, J.A., Perpinan

606   Lamigueiro, O., Bevan, A., Racine, E.B., Shortridge, A. & Ghosh, A. (2017) Package 'raster':

607   Geographic Data Analysis and Modeling. Available at: https://cran.r-

608   project.org/web/packages/raster/raster.pdf.

609   Jiménez, L., Soberón, J., Christen, J.A. & Soto, D. (2019) On the problem of modeling a fundamental

610   niche from occurrence data. *Ecological Modelling*, **397**, 74–83.

611   Kjellström, E., Nikulin, G., Strandberg, G., Christensen, O.B., Jacob, D., Keuler, K., Lenderink, G., van

612   Meijgaard, E., Schär, C., Somot, S., Sørland, S.L., Teichmann, C. & Vautard, R. (2018) European

613   climate change at global mean temperature increases of 1.5 and 2 degrees C above pre-industrial

614   conditions as simulated by the EURO-CORDEX regional climate models. *Earth System Dynamics*,

615   **9**, 459–478.

616   Kollas, C., Körner, C. & Randin, C.F. (2014) Spring frost and growing season length co-control the cold

617   range limits of broad-leaved trees. *Journal of Biogeography*, **41**, 773–783.

618   Kramer, K., Degen, B., Buschbom, J., Hickler, T., Thuiller, W., Sykes, M.T. & de Winter, W. (2010)

619   Modelling exploration of the future of European beech (Fagus sylvatica L.) under climate change-

620   Range, abundance, genetic diversity and adaptive response. *Forest Ecology and Management*, **259**,

621   2213–2222.

622   Laughlin, D.C. (2018) Rugged fitness landscapes and Darwinian demons in trait-based ecology. *New

623   Phytologist*, **217**, 501–503.

624   Laughlin, D.C. & Messier, J. (2015) Fitness of multidimensional phenotypes in dynamic adaptive

625   landscapes. *Trends in Ecology & Evolution*, **30**, 487–496.

626 Leites, L.P., Robinson, A.P., Rehfeldt, G.E., Marshall, J.D. & Crookston, N.L. (2012) Height-growth

627 response to changes in climate differ among populations of interior Douglas-fir: a novel analysis of

628 provenance-test data. *Ecological Applications*, **22**, 154–165.

629 Ma, Q., Huang, J., Hänninen, H. & Berninger, F. (2018) Agricultural and Forest Meteorology Reduced

630 geographical variability in spring phenology of temperate trees with recent warming. *Agricultural*

631 *and Forest Meteorology*, **256**–**257**, 526–533.

632 Mátyás, C. (1999) Forest genetics and sustainability. *Dordrecht, Boston: Kluwer Academic Publishers*.

633 Mazerolle, M.J. (2006) Improving data analysis in herpetology: Using Akaike's information criterion

634 (AIC) to assess the strength of biological hypotheses. *Amphibia Reptilia*, **27**, 169–180.

635 Merow, C., Bois, S.T., Allen, J.M., Xie, Y. & Silander, J.A. (2017) Climate change both facilitates and

636 inhibits invasive plant ranges in New England. *Proceedings of the National Academy of Sciences*,

637 **114**, E3276–E3284.

638 Mitchell, R.M. & Bakker, J.D. (2014) Intraspecific Trait Variation Driven by Plasticity and Ontogeny in

639 Hypochaeris radicata. *PLoS ONE*, **9**.

640 Nazarenko, L., G. A. Schmidt, R. L. Miller, N. Tausnev, M. Kelley, R. Ruedy, G.L.R., I. Aleinov, M.

641 Bauer, S. Bauer, R. Bleck, V. Canuto, Y. Cheng, T. L. Clune, a. D.D.G., G. Faluvegi, J. E. Hansen,

642 R. J. Healy, N. Y. Kiang, D. Koch, A. A. Lacis, a. N.L., J. Lerner, K. K. Lo, S. Menon, V. Oinas, J.

643 Perlwitz, M. J. Puma, D. Rind, a. R., M. Sato, D. T. Shindell, S. Sun, K. Tsigaridis, N. Unger, A.

644 Voulgarakis, M.-S.Y. & Zhang, and J. (2015) Future climate change under RCP emission scenarios

645 with GISS ModelE2. *Journal of Advances in Modeling Earth Systems*, 244–268.

646 Paradis, E., Blomberg, S., Bolker, B., Brown, J., Claude, J., Cuong, H.S., Desper, R., Didier, G., Durand,

647 B., Dutheil, J., Ewing, R., Gascuel, O., Guillerme, T., Heibl, C., Ives, A., Jones, B., Krah, F.,

648 Lawson, D., Lefort, V., Legendre, P., Lemon, J., Marcon, E., McCloskey, R., Nylander, J., Opgen-

649 Rhein, R., Popescu, A.-A., Royer-Carenzi, M., Schliep, K., Strimmer, K. & Vienne, D. de (2018)

650   Package 'ape' : Analyses of Phylogenetics and Evolution. Available at: https://cran.r-

651   project.org/web/packages/ape/ape.pdf.

652   Pedlar, J.H. & McKenney, D.W. (2017) Assessing the anticipated growth response of northern conifer

653   populations to a warming climate. *Scientific Reports*, **7**, 1–10.

654   Peterson, M.L., Doak, D.F. & Morris, W.F. (2018) Both life-history plasticity and local adaptation will

655   shape range-wide responses to climate warming in the tundra plant Silene acaulis. *Global Change*

656   *Biology*, **24**, 1614–1625.

657   Pflug, E.E., Buchmann, N., Siegwolf, R.T.W., Schaub, M., Rigling, A. & Arend, M. (2018) Resilient

658   Leaf Physiological Response of European Beech (Fagus sylvatica L.) to Summer Drought and

659   Drought Release. *Frontiers in Plant Science*, **9**, 187.

660   Purves, D.W. (2009) The demography of range boundaries versus range cores in eastern US tree species.

661   *Proceedings of the Royal Society B: Biological Sciences*, **276**, 1477–1484.

662   R Development Core Team, R. (2015) R: A Language and Environment for Statistical Computing. R

663   Foundation for Statistical Computing, Vienna, Austria. Avaliable at: http://www.Rproject. org.

664   Reich, P.B., Sendall, K.M., Stefanski, A., Wei, X., Rich, R.L. & Montgomery, R.A. (2016) Boreal and

665   temperate trees show strong acclimation of respiration to warming. *Nature*, **531**, 633–636.

666   Richardson, B.A., Chaney, L., Shaw, N.L. & Still, S.M. (2017) Will phenotypic plasticity affecting

667   flowering phenology keep pace with climate change? *Global Change Biology*, **23**, 2499–2508.

668   Robson, T.M., Alia, R., Bozic, G., Clark, J., Forsteuter, M., Gomory, D., Liesebach, M., Mertens, P.,

669   Rasztovits, E., Zitová, M. & von Wühlisch, G. (2011) The timing of leaf flush in European beech

670   (Fagus sylvatica L.) saplings. *Genetic Resources of European Beech (Fagus sylvatica L.) for*

671   *Sustainable Forestry: Proceedings of the COST E52 Final Meeting. SERIE FORESTAL*, **22**, 61–80.

672   Robson, T.M., Benito Garzón, M. & BeechCOSTe52 database consortium (2018) Data Descriptor:

673   Phenotypic trait variation measured on European genetic trials of Fagus sylvatica L. *Scientific Data*,

674   **5**, 1–7.

675   Robson, T.M., Rasztovits, E., Aphalo, P.J., Alia, R. & Aranda, I. (2013) Flushing phenology and fitness

676   of European beech (Fagus sylvatica L.) provenances from a trial in La Rioja, Spain, segregate

677   according to their climate of origin. *Agricultural and Forest Meteorology*, **180**, 76–85.

678   Des Roches, S., Post, D.M., Turley, N.E., Bailey, J.K., Hendry, A.P., Kinnison, M.T., Schweitzer, J.A. &

679   Palkovacs, E.P. (2018) The ecological importance of intraspecific variation. *Nature Ecology &*

680   *Evolution*, **2**, 57–64.

681   Saltré, F., Duputié, A., Gaucherel, C. & Chuine, I. (2015) How climate, migration ability and habitat

682   fragmentation affect the projected future distribution of European beech. *Global Change Biology*,

683   **21**, 897–910.

684   Savolainen, O., Pyhäjärvi, T. & Knürr, T. (2007) Gene Flow and Local Adaptation in Trees. *Annual*

685   *Review of Ecology, Evolution, and Systematics*, **38**, 595–619.

686   Scheepens, J.F., Deng, Y. & Bossdorf, O. (2018) Phenotypic plasticity in response to temperature

687   fluctuations is genetically variable, and relates to climatic variability of origin, in Arabidopsis

688   thaliana. *AoB PLANTS*, **10**, 1–12.

689   Stahl, U., Reu, B. & Wirth, C. (2014) Predicting species' range limits from functional traits for the tree

690   flora of North America. *Proceedings of the National Academy of Sciences*, **111**, 13739–13744.

691   Stojnic, S., Suchocka, M., Benito-Garzon, M., Torres-Ruiz, J., Cochard, H., Bolte, A., Cocozza, C.,

692   Cvjetkovic, B., de Luis, M., Martinez-Vilalta, J., Raebild, A., Tognetti, R. & Delzon, S. (2018)

693   Variation in xylem vulnerability to embolism in European beech from geographically marginal

694   populations Variation in xylem vulnerability to embolism in European beech from geographically

695   marginal populations. *Tree Physiology*, **38**, 173–185.

696   Svenning, J.C. & Skov, F. (2005) The relative roles of environment and history as controls of tree species

697   composition and richness in Europe. *Journal of Biogeography*, **32**, 1019–1033.

698 Trumbore, S., Brando, P. & Hartmann, H. (2015) Forest health and global change. *Science*, **349**, 814–818.

699 Urban, M.C., Bocedi, G., Hendry, A.P., Mihoub, J.B., Pe'er, G., Singer, A., Bridle, J.R., Crozier, L.G.,

700 De Meester, L., Godsoe, W., Gonzalez, A., Hellmann, J.J., Holt, R.D., Huth, A., Johst, K., Krug,

701 C.B., Leadley, P.W., Palmer, S.C.F., Pantel, J.H., Schmitz, A., Zollner, P.A. & Travis, J.M.J. (2016)

702 Improving the forecast for biodiversity under climate change. *Science*, **353**.

703 Valladares, F., Matesanz, S., Guilhaumon, F., Araújo, M.B., Balaguer, L., Benito-Garzón, M., Cornwell,

704 W., Gianoli, E., van Kleunen, M., Naya, D.E., Nicotra, A.B., Poorter, H. & Zavala, M.A. (2014) The

705 effects of phenotypic plasticity and local adaptation on forecasts of species range shifts under

706 climate change. *Ecology Letters*, **17**, 1351–1364.

707 Vautard, R., Gobiet, A., Sobolowski, S., Kjellström, E., Stegehuis, A., Watkiss, P., Mendlik, T.,

708 Landgren, O., Nikulin, G., Teichmann, C. & Jacob, D. (2014) The European climate under a 2 ◦ C

709 global warming. *Environmental Research Letters*, **9**, 1–11.

710 Vitasse, Y., Lenz, A., Hoch, G. & Korner, C. (2014) Earlier leaf-out rather than difference in freezing

711 resistance puts juvenile trees at greater risk of damage than adult trees. *Journal of Ecology*, **102**,

712 981–988.

713 Volaire, F. (2018) A unified framework of plant adaptive strategies to drought: crossing scales and

714 disciplines. *Global Change Biology (in press)*.

715 Way, D.A. & Montgomery, R.A. (2015) Photoperiod constraints on tree phenology, performance and

716 migration in a warming world. *Plant, Cell & Environment*, **38**, 1725–1736.

717 Younginger, B.S., Sirová, D., Cruzan, M.B. & Ballhorn, D.J. (2017) Is Biomass a Reliable Estimate of

718 Plant Fitness? *Applications in Plant Sciences*, **5**, 1600094.

719

720

1
2
3
4
5
6
7
8
9
10
11
12
13
14
15
16
17
18
19
20
21
22
23
24
25
26
27
28
29
30
31
32
33
34
35
36
37
38
39
40
41
42
43
44
45
46
47
48
49
50
51
52
53
54
55
56
57
58
59
60

721   **DATA ACCESSIBILITY**

722   All phenotypic data used in this study are available at

723   https://zenodo.org/record/1240931#.XBuSa81CeUk (Robson *et al.*, 2018). All the maps

724   generated in this study are available from the authors.

725

726

727

728

729

730

731

732

733

734

735

736

737

738

739

740

741   **Tables & Figures**

742   **Figure 1.** Map: Distribution range of *Fagus sylvatica* L. (shaded in beige) and location of the

743   provenances and trials by trait. Circles indicate the location of the provenances and triangles that

744   of the trials. Different colors have been employed to indicate the different traits (VG: vertical

745   growth; RG: radial growth; YTS: young tree survival; LF: leaf flushing). Table: The extent of data

746   from the BeechCOSTe52 database (Robson et al. 2018) used for modelling. Measurements: total

747   number of measurements; Trees: total number of individual trees; Trials: total number of trials;

748   Provenances: total number of provenances, Age: the age at which the trees were measured.

749   Columns indicate sample sizes for the traits used in the one-trait models and in the two-trait

750   models.

	VG	RG	YTS	LF	H-RG	H-LF
Measurements	203 105	34 237	41 309	7 863	34 237	12 087
Trees	108 415	31 339	37 433	7 863	31 339	10 634
Trials	36	19	7	7	19	6
Provenances	205	186	114	62	186	150
Age	2 to 15	8 to 15	2 to 6	12	8 to 15	6, 9, 11, 12, 15

751

752

753

754

755

756

757   **Table 1.** Summary of the variables included in the final best-supported models (one- and two-trait)

758   for each trait analyzed. Environmental variables selected for the provenances and the trials for the

759   one-trait models of height, DBH, young tree survival and flushing, and for the two-trait models of

760   height-DBH and height-leaf flushing. H: height; DBH: diameter at breast height; Lf: leaf flushing;

761   PET Max: maximal monthly potential evapotranspiration; BIO12: annual precipitation; BIO13:

762   precipitation of wettest month; BIO14: precipitation of driest month; MTdjf: mean temperature of

763   December, January and February; Co-variate: trait covariate.

764

		one-trait models				two-trait models	
		Height	**DBH**	**Young tree survival**	**Leaf flushing**	**H-DBH**	**H-Lf**
Variables	**Environment of the provenance**	PET Max	PET Max	PET Max	MTdjf Latitude	PET Max	PET Max
	Environment of the trial	BIO13	BIO12	BIO14	MTdjf Latitude Longitude	BIO13	BIO13
	Co-variate					DBH	Lf

765

766

767

768

769

770

771

772 **Table 2.** Summary statistics for a generalized linear model (binomial family) of beech occurrence

773 (presence/absence) as a function of trait spatial predictions and their interactions. Estimate:

774 coefficient of the regression shown on a logarithmic scale; SE: standard error of fixed variables; t:

775 Wald statistical test that measures the point estimate divided by the estimate of its standard error,

776 assuming a Gaussian distribution of observations; p: p-value; DE: deviance explained; VG:

777 vertical growth; RG: radial growth; YTS: young tree survival; LF: leaf flushing.

|	Estimate	SE	t	p	DE
(Intercept)	-5.84	1.15e-02	-509.03	2.00E-16	
VG	5.45	1.64e-02	332.93	2.00E-16	0.37
RG	0.51	7.93e-03	64.67	2.00E-16	0.33
YTS	2.11	3.75e-03	562.83	2.00E-16	0.19
LG	3.12	1.48e-02	210.94	2.00E-16	0.01
VG x YTS	0.10	4.30e-03	21.08	2.00E-16	0.03
RG x YTS	-0.60	2.04e-03	-295.94	2.00E-16	0.01
YTS x LF	-1.40	4.02e-03	-348.1	2.00E-16	0.01
VG x RG	-1.11	4.62e-03	-240.58	2.00E-16	0.01
VG x LF	-7.81	2.15e-02	-363.18	2.00E-16	0.01
RG x LF	3.43	1.09e-02	313.89	2.00E-16	0.02
Model total deviance					**0.31**

778

779

780

781

782

783

784 **Figure 2.** Spatial projections for (a) vertical growth (cm), (b) radial growth (mm), (c) young tree

785 survival (probability) and (d) leaf flushing (Julian days) generated using one-trait models (maps

786 on the left), and corresponding graphs of interactions between the best environmental predictor

787 variable across the trials divided according to environment at the provenance for each of the four

788 traits (graphs on the right). Interactions represent the differences in trait values that can be

789 attributed to the provenance (interpretable as local adaptation driven by PET max in (a), (b), and

790 (c) and driven by the latitude in (d)). Interactions also represent the differences in trait values that

791 can be attributed to the environmental conditions of trial (interpretable as phenotypic plasticity

792 driven by the environmental variables shown in the x-axis). Black, dark grey, and light grey lines

793 represent high, medium and low values of the climatic variable of the provenances (as opposed to

794 those of the trial, indicated on the x-axis). The vertical lines represent the confidence intervals.

795 The maps display the trait projection for contemporary climate (inferred from 2000-2014

796 meteorological data) across the current species range. The color gradient depicts the clinal

797 variation from low (red) to high (blue) values of each trait. The values of the different traits are

798 represented in the following way: vertical growth (cm), radial growth (mm), probability of young

799 tree survival (0 =dead, 1=alive) and leaf flushing (Julian days). PET max prov: maximal monthly

800 potential evapotranspiration at the provenance; Latitude prov: latitude of the provenance.
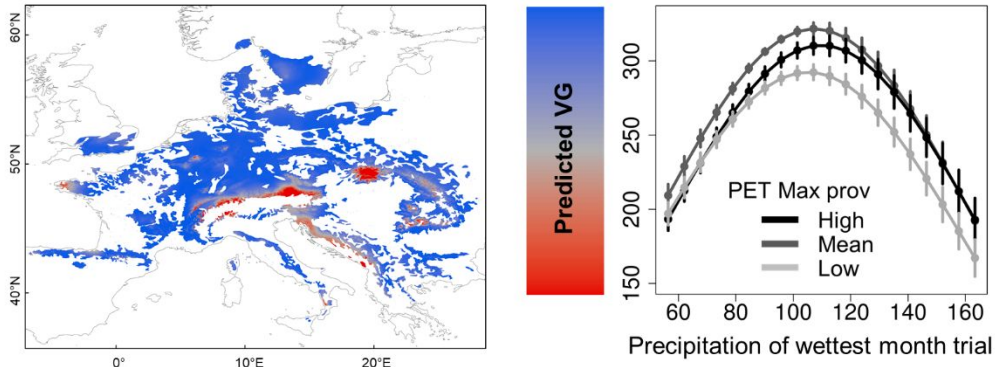
(a) Vertical growth

(b) Radial growth
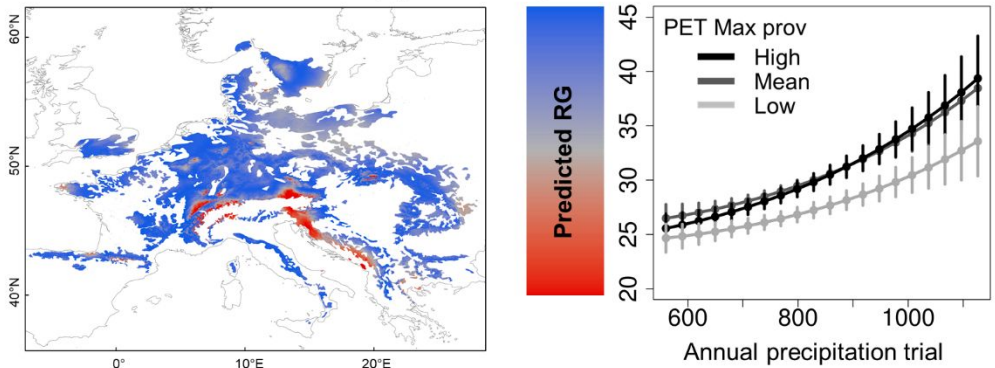
(c) Young tree survival

(d) Leaf flushing

801

802
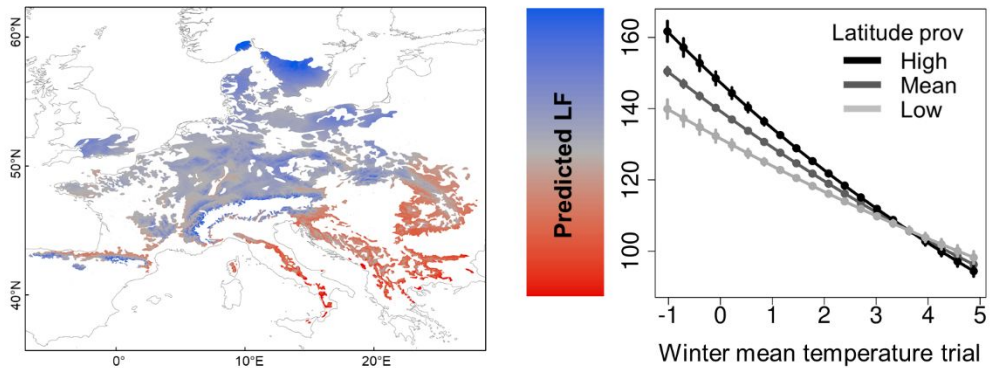
803 **Figure 3.** Spatial projections of vertical growth (cm) for (a) Vertical-radial growth model and (b)

804 vertical growth-leaf flushing models (maps on the left), and the corresponding graphs of co-

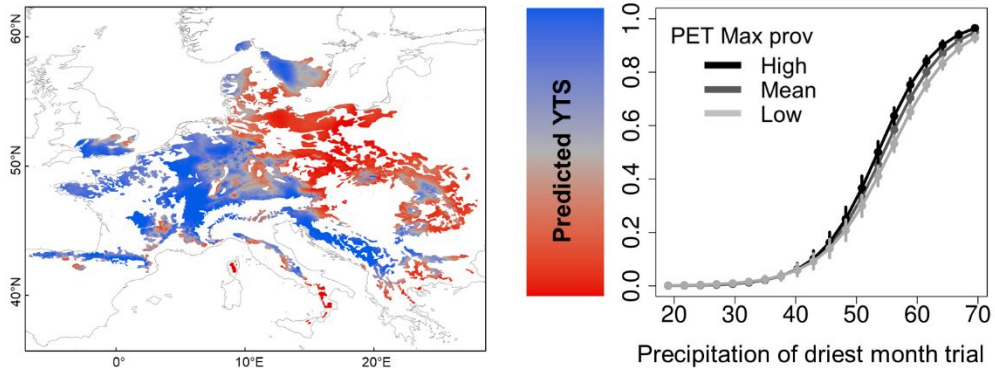805 variation between vertical growth and the covariate: (a) DBH (mm) and (b) leaf flushing (Julian

806 days). Black, dark grey, and light grey lines represent high, medium and low values of the

807 precipitation of the wettest month of the trial (BIO13). The vertical lines represent the confidence

808 intervals. The maps display the trait projection for contemporary climate (inferred from 2000-2014

809 meteorological data) across the current species range. The color gradient depicts the clinal

810 variation in vertical growth from 200 cm (gray) to 600 cm (blue).

(a) Vertical growth-radial growth

(b) Vertical growth-leaf flushing

Figure 4. Spatial predictions for 2070 (RCP 8.5) across the species range for one-trait models: (a) vertical growth (cm); (b) radial growth (mm); (c) probability of young tree survival (0=dead; 1=alive); (d) leaf flushing (Julian days); and for two-trait models: (e) vertical growth (cm; co-variate radial growth) and (f) vertical growth (cm; co-variate leaf flushing). The color gradients depict the clinal variation from low (red) to high (blue) values.

APPENDIX S1: Supporting information

1. Moran's I correlation coefficient

Supporting Information Table S1.1. Statistics of the spatial autocorrelation of vertical growth (VG), radial growth (RG), young tree survival (YTS) and leaf flushing (LF). Ob: observed computed Moran's I; Ex: expected value of I under the null hypothesis; Sd: standard deviation of I under the null hypothesis; p-value: p-value of the test of the null hypothesis against the alternative hypothesis; Null hypothesis: the data does not have spatial correlation.

	VG	RG	YTS	LF
Ob	-0.04	-0.09	-0.17	-0.10
Ex	-0.03	-0.05	-0.13	-0.08
Sd	0.06	0.06	0.17	0.08
p-value	0.81	0.47	0.78	0.74

2. Moran's I correlograms
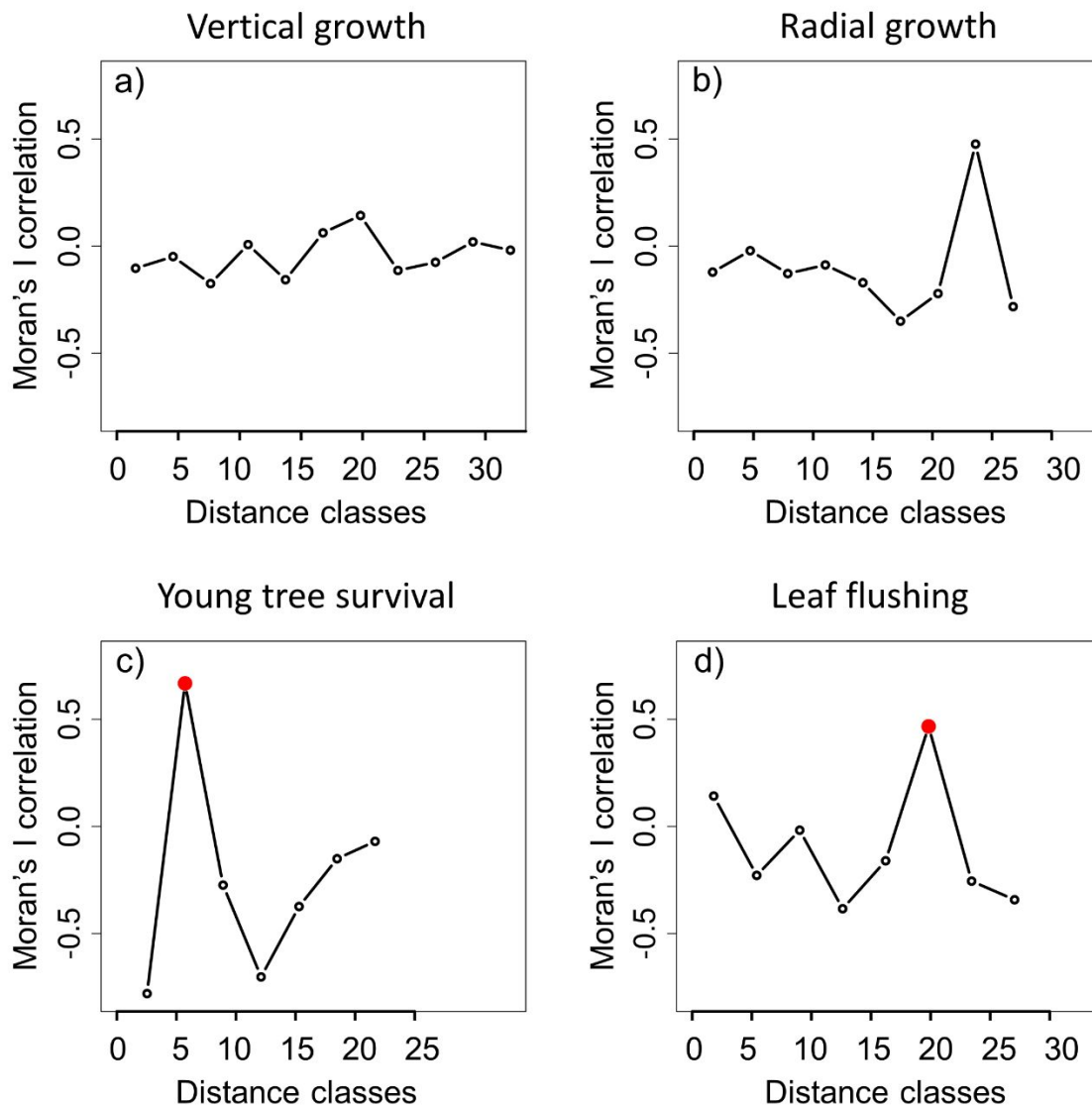
Supporting Information Figure S1.1. Correlograms of Moran's I correlation coefficient (y-axis) and the distance classes (x-axis) for vertical (a) and radial (b) growth, young tree survival (c), and leaf flushing (d). Moran's correlation coefficient ranges between 1 and -1. Distance classes are Euclidian and in degrees. Distances of significant spatial dependence are shown in red (significant values $p < 0.05$).

1
2
3
4
5
6
7
8
9
10
11
12
13
14
15
16
17
18
19
20
21
22
23
24
25
26
27
28
29
30
31
32
33
34
35
36
37
38
39
40
41
42
43
44
45
46
47
48
49
50
51
52
53
54
55
56
57
58
59
60

3. Climatic variables

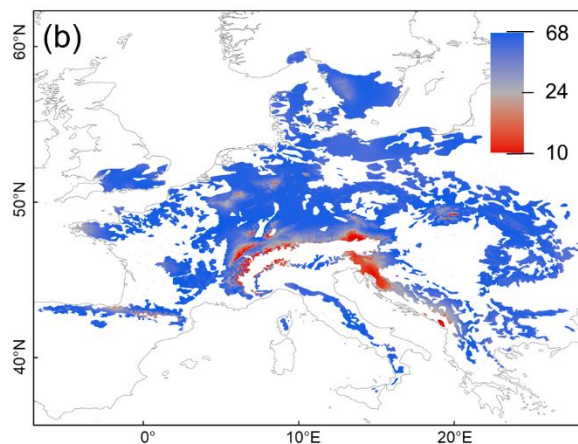**Supporting Information Table S1.2.** List of yearly climatic variables provided by EuMedClim.

°C: Celsius degree; mm: millimeters; water balance: precipitation minus potential evapotranspiration.

| Climatic variables	Definition	Unit
BIO1	Annual mean temperature	°C
BIO2	Mean diurnal temperature range	°C
BIO5	Maximal temperature of the warmest month	°C
BIO6	Minimal temperature of the coldest month	°C
BIO12	Annual precipitation	mm
BIO13	Precipitation of the wettest month	mm
BIO14	Precipitation of the driest month	mm
MTdjf	Mean temperature of December, January and February	°C
MTmam	Mean temperature of March, April and May	°C
MTjaj	Mean temperature of June, July and August	°C
MTson	Mean temperature of September, October and November	°C
Pdjf	Precipitation of December, January and February	mm
Pmam	Precipitation of March, April and May	mm
Pjaj	Precipitation of June, July and August	mm
Pson	Precipitation of September, October and November	mm
PET Mean	Annual potential evapotranspiration	mm
PET Max	Maximal monthly potential evapotranspiration	mm
PET Min	Minimal monthly potential evapotranspiration	mm
PPET Mean	Annual water balance	mm
PPET Max	Maximal monthly water balance	mm
PPET Min	Minimal monthly water balance	mm

4. Principal Components Analysis (PCA) of the climate variables
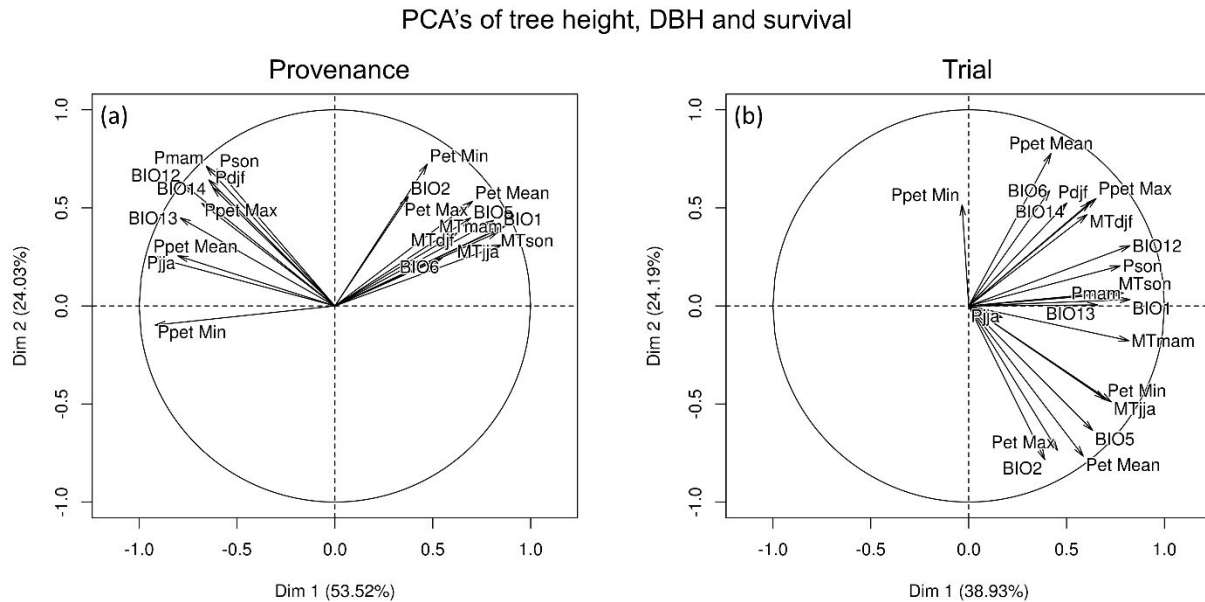
PCA's of tree height, DBH and survival

Supporting Information Figure S1.2. Results of PCA for checking for co-linearity and reducing the climatic space to select the final climate variables for the stepwise procedure used in the models on traits vertical and radial growth, and young tree survival, conducted by provenance (a) and by trial (b). When two variables are strongly correlated, only one of them was used in models. The variance explained by the first two axes is indicated in the figures.

5. AIC analysis

We performed a total of 64 one-trait models and selected the best model based on AIC.

Supporting Information Table S1.3. AIC values obtained for vertical growth, radial growth, young tree survival and leaf flushing one-trait models. AIC: Akaike information criterion; CP: climate of the provenance; CT: climate of the trial; BIO1: annual mean temperature; BIO5: max temperature of warmest month; BIO6: min temperature of coldest month; BIO12: annual precipitation; BIO13: precipitation of wettest month; BIO14: precipitation of driest month; PET Max: maximal monthly potential evapotranspiration; PET Mean: annual potential evapotranspiration; MTdjf: mean temperature of December, January and February; MTmam: mean temperature of March, April and May; MTjja: mean temperature of June, July and August; MTson: mean temperature of September, October and November; MTdjfmam: mean temperature of December, January, February March, April and May.

Vertical growth			Radial growth			Young tree survival			Leaf flushing		
CP	CT	AIC	CP	CT	AIC	CP	CT	AIC	CP	CT	AIC
PET Max	BIO13	102495.10	PET Max	BIO12	23099.69	PET Max	BIO14	39299.61	MTdjf	MTdjf	-32835.88
BIO13	BIO13	102498.40	BIO12	BIO12	23099.77	BIO5	PET Max	39299.75	MTdjfmam	BIO5	-32835.2
BIO1	BIO13	102509.20	PET Mean	BIO12	23100.00	BIO5	BIO13	39300.20	MTdjfmam	MTdjf	-32835.01
BIO5	BIO13	102509.70	BIO5	BIO12	23100.17	BIO14	BIO14	39300.57	MTdjf	BIO5	-32834.71
PET Mean	BIO13	102515.30	BIO13	BIO12	23105.95	PET Mean	PET Max	39301.21	BIO1	MTdjf	-32833.53
BIO12	BIO13	102538.90	BIO14	BIO12	23107.76	PET Mean	BIO14	39303.74	MTson	MTdjf	-32833.2
BIO6	BIO13	102647.10	BIO1	BIO12	23109.40	PET Max	PET Max	39307.04	BIO1	BIO5	-32832.97
BIO14	BIO13	102694.40	BIO14	PET Max	23112.39	BIO12	BIO14	39307.83	MTdjfmam	MTjja	-32832.95
BIO5	BIO12	102827.20	BIO6	BIO12	23113.15	BIO5	BIO12	39308.26	BIO6	MTdjf	-32832.8
BIO1	BIO12	102836.50	PET Max	PET Max	23119.66	BIO13	BIO13	39308.30	MTdjf	MTjja	-32832.59
PET Max	BIO12	102849.60	BIO12	PET Max	23119.73	PET Mean	BIO1	39308.32	MTson	BIO5	-32832.53
PET Mean	BIO12	102849.80	PET Mean	PET Max	23123.73	BIO5	BIO14	39308.80	BIO6	BIO5	-32831.78
BIO13	BIO12	102856.00	BIO13	PET Max	23124.58	PET Mean	PET Mean	39308.84	BIO1	MTjja	-32830.75
BIO12	BIO12	102924.80	BIO5	PET Max	23127.81	BIO5	BIO1	39308.93	MTson	MTjja	-32830.39
BIO6	BIO12	103000.30	BIO6	PET Max	23129.06	BIO5	PET Mean	39309.13	MTmam	MTdjf	-32829.82
BIO14	BIO12	103035.00	BIO1	PET Max	23131.01	BIO13	PET Max	39310.60	MTmam	BIO5	-32829.69
BIO13	BIO14	104366.60	PET Mean	BIO13	23155.46	PET Mean	BIO5	39310.84	BIO6	MTjja	-32829.67

BIO12	BIO14	104433.70	BIO1	BIO13	23158.17	BIO13	BIO14	39311.05	MTdjfmam	MTson	-32828.93
BIO5	BIO5	104479.60	BIO5	BIO13	23158.45	PET Mean	BIO13	39311.74	MTdjf	MTson	-32828.49
BIO1	BIO5	104486.20	PET Max	BIO13	23160.20	PET Max	BIO13	39312.16	MTmam	MTjja	-32827.31
BIO13	BIO5	104486.40	BIO6	BIO13	23161.55	BIO13	BIO12	39312.17	BIO1	MTson	-32826.31
PET Max	BIO5	104498.00	BIO12	BIO13	23170.84	BIO6	BIO13	39312.88	BIO5	BIO5	-32826.25
PET Mean	BIO5	104502.00	BIO14	BIO13	23170.94	PET Max	BIO1	39313.22	MTson	MTson	-32825.79
BIO12	BIO5	104531.00	BIO13	BIO13	23172.87	BIO14	BIO13	39313.52	BIO6	MTson	-32825.65
BIO1	BIO14	104548.20	BIO12	BIO14	23213.00	BIO5	BIO6	39313.96	BIO5	MTdjf	-32825.32
BIO6	BIO5	104551.90	BIO13	BIO14	23214.59	BIO12	PET Max	39314.37	BIO5	MTjja	-32824.01
PET Max	BIO14	104554.10	BIO14	BIO14	23221.30	BIO12	BIO13	39314.57	MTmam	MTson	-32823.39
PET Mean	BIO14	104561.80	PET Max	BIO14	23228.03	BIO13	BIO1	39314.63	MTdjfmam	BIO1	-32821.39
BIO5	BIO14	104568.60	BIO12	BIO6	23228.43	BIO5	BIO5	39315.15	MTdjf	BIO1	-32821.3
BIO14	BIO5	104595.80	PET Mean	BIO14	23229.18	PET Max	PET Mean	39315.57	BIO5	MTson	-32819.16
BIO14	BIO14	104632.90	BIO13	BIO6	23230.85	BIO1	BIO13	39315.98	BIO1	BIO1	-32818.88
BIO6	BIO14	104662.10	BIO5	BIO14	23231.28	BIO1	BIO14	39316.04	MTson	BIO1	-32818.63
BIO5	BIO1	104948.50	BIO6	BIO14	23231.86	BIO6	BIO14	39316.50	MTjja	BIO5	-32818.54
PET Max	BIO1	104951.50	BIO1	BIO14	23235.69	BIO12	BIO1	39316.56	BIO6	BIO1	-32818.38
PET Mean	BIO1	104953.40	BIO14	BIO6	23236.45	PET Mean	BIO12	39316.71	MTjja	MTdjf	-32817.94
BIO13	BIO1	104958.20	BIO6	BIO6	23240.51	BIO6	BIO12	39316.72	MTjja	MTjja	-32816.41
BIO1	BIO1	104990.00	PET Max	BIO6	23247.34	BIO6	PET Max	39316.79	MTmam	BIO1	-32815.09
BIO12	BIO1	105034.80	PET Mean	BIO6	23248.79	PET Max	BIO12	39316.82	MTdjfmam	BIO6	-32813.73
BIO6	BIO1	105103.40	BIO5	BIO6	23251.22	BIO13	PET Mean	39317.10	MTdjf	BIO6	-32813.64
BIO14	BIO1	105134.00	BIO1	BIO6	23251.39	PET Max	BIO6	39317.35	MTson	BIO6	-32811.78
BIO13	PET Mean	105607.20	PET Max	BIO5	23326.60	BIO1	PET Max	39317.45	BIO1	BIO6	-32811.7
BIO13	BIO6	105655.60	PET Mean	BIO5	23330.74	PET Max	BIO5	39317.56	MTjja	MTson	-32811.33
BIO12	PET Mean	105700.20	BIO5	BIO5	23333.80	BIO13	BIO6	39317.60	BIO6	BIO6	-32810.51
BIO12	BIO6	105740.90	BIO14	BIO5	23336.46	PET Mean	BIO6	39317.70	BIO5	BIO1	-32810.39
BIO5	PET Mean	105752.70	BIO12	BIO5	23337.86	BIO1	BIO1	39317.71	MTmam	BIO6	-32807.09
BIO1	PET Mean	105753.10	BIO13	BIO5	23342.73	BIO14	PET Max	39317.82	MTjja	BIO1	-32803.17
PET Max	PET Mean	105762.50	BIO1	BIO5	23343.08	BIO14	BIO1	39317.95	BIO5	BIO6	-32803.03
PET Mean	PET Mean	105769.40	BIO12	BIO1	23344.66	BIO14	BIO12	39318.04	MTdjfmam	MTdjfmam	-32798.69
PET Max	BIO6	105777.20	PET Max	BIO1	23345.37	BIO12	BIO12	39318.24	MTdjf	MTdjfmam	-32798.47
PET Mean	BIO6	105777.90	BIO6	BIO5	23345.84	BIO6	BIO1	39318.36	MTson	MTdjfmam	-32796.38
BIO5	BIO6	105782.20	BIO5	BIO1	23349.97	BIO13	BIO5	39318.74	BIO1	MTdjfmam	-32796.37
BIO1	BIO6	105790.00	PET Mean	BIO1	23350.61	BIO12	BIO6	39320.02	MTjja	BIO6	-32795.95
BIO6	PET Mean	105851.70	BIO14	BIO1	23353.91	BIO12	PET Mean	39320.05	BIO6	MTdjfmam	-32795.67
BIO14	PET Mean	105867.10	BIO13	BIO1	23354.27	BIO14	BIO6	39320.34	MTmam	MTdjfmam	-32792.13
BIO6	BIO6	105898.10	BIO6	BIO1	23363.77	BIO6	BIO6	39320.41	BIO5	MTdjfmam	-32787
BIO14	BIO6	105901.40	BIO1	BIO1	23367.18	BIO12	BIO5	39320.73	MTdjfmam	MTmam	-32786.71
BIO13	PET Max	106062.80	BIO14	PET mean	23417.15	BIO1	BIO6	39321.01	MTdjf	MTmam	-32785.98
BIO12	PET Max	106132.40	PET Max	PET mean	23420.69	BIO1	BIO12	39321.06	BIO1	MTmam	-32784.65
BIO1	PET Max	106176.20	BIO12	PET mean	23423.00	BIO1	PET Mean	39321.28	MTson	MTmam	-32784.57
BIO5	PET Max	106179.00	PET Mean	PET mean	23423.23	BIO6	PET Mean	39321.81	BIO6	MTmam	-32783.62
PET Max	PET Max	106187.20	BIO5	PET mean	23426.95	BIO14	PET Mean	39321.88	MTmam	MTmam	-32780.58
PET Mean	PET Max	106194.00	BIO13	PET mean	23427.90	BIO14	BIO5	39322.35	MTjja	MTdjfmam	-32780.05
BIO14	PET Max	106256.90	BIO6	PET mean	23431.24	BIO1	BIO5	39323.48	BIO5	MTmam	-32775.52
BIO6	PET Max	106268.70	BIO1	PET mean	23432.28	BIO6	BIO5	39323.84	MTjja	MTmam	-32768.2

6. Summary statistics of one-trait models

Supporting Information Table S1.4. Statistics of random and fixed effects from generalized linear mixed-effect models of vertical growth, radial growth, young tree survival and leaf flushing. Obs: number of trait measurements; Variance: variance explained by the random effects; SD: standard deviation of each level of random effects; Estimate: coefficient of the regression, shown on a logarithmic scale for vertical growth, radial growth and leaf flushing; SE: standard error of each fixed variable; t: Wald statistical test that measures the point estimate divided by the estimate of its SE, assuming a Gaussian distribution of observations conditional on fixed and random effects; z: Wald statistical test that measures the point estimate divided by the estimate of its SE, assuming a binomial distribution of observations conditional on fixed and random effects. Fixed effects: Coefficients of the fixed effects of the model; CP: climate of the provenance origin; CT: climate of the trial; LatP: latitude of the provenance origin; LatT: latitude of the trial; LongT: longitude of the trial; CP^2: quadratic effect of the climate of the provenance; CT^2: quadratic effect of the climate of the trial. Coefficients of the interactions: Age x CP, Age x CT, CP x CT, LatP x CT, LatP x LatT, LatP x LongT, CP x LongT. R^2M: percentage of the variance explained by the fixed effects (Marginal variance); R^2C: percentage of the variance explained by the random and fixed effects (Conditional variance); r: Pearson correlation. The climate variable of the provenance (CP) for vertical growth, radial growth and young tree survival is maximal potential evapotranspiration; CP for leaf flushing is mean temperature of December, January and February. The climate variable of the trial (CT) for vertical growth is precipitation of the wettest month, for radial growth is annual precipitation, for young tree survival is precipitation of the driest month and for leaf flushing is mean temperature of December, January and February.

	Vertical growth			Radial growth			Young tree survival			Leaf flushing		
Model	Linear Mixed Effect			Linear Mixed Effect			Generalized Linear Mixed Effect (Family: binomial)			Linear Mixed Effect		
	Random Effects			Random Effects			Random Effects			Random Effects		
	Obs	Variance	SD	Obs	Variance	SD	Obs	Variance	SD	Obs	Variance	SD
Provenance	205	1.00e-02	9.00e-02	187	9.31e-03	9.65e-02	114	2.98e-01	5.46e-01	62	4.60e-04	2.20e-02
Trial	36	9.00e-02	3.00e-01	19	3.81e-01	6.17e-01	7	6.31e-01	7.94e-01	7	3.60e-05	6.00e-03
Trial:Block	107	9.00e-02	1.00e-01	56	6.97e-03	8.35e-02	21	1.48e-01	3.84e-01			
Trial:Block:Tree	108415	8.00e-02	2.80e-01	31339	1.10e-01	3.32e-01	37433	1.16e-02	1.08e-01			
Residuals		5.00e-02	2.20e-01		1.66e-02	1.29e-01		1.54e-01	3.92e-01		8.56e-04	2.92e-02
	Fixed Effects			Fixed Effects			Fixed Effects			Fixed Effects		
	Estimate	SE	t	Estimate	SE	t	Estimate	SE	z	Estimate	SE	t
Intercept	4.84e+00	5.22e-02	92.7	2.82e+00	1.56e-01	18.1	1.08e+00	3.38e-01	3.2	4.76e+00	5.16e-03	921.9
Age	6.45e-01	1.14e-03	563.6	7.17e-01	8.74e-03	82	-1.72e+00	9.29e-02	-18.5			
CP	2.58e-02	6.93e-03	3.7	2.94e-02	8.81e-03	3.3	2.83e-02	5.30e-02	0.1	1.07e-02	2.63e-03	4.1
CT	9.70e-02	4.63e-03	20.9	2.54e-01	7.02e-02	3.6	1.54e-01	2.78e-01	0.6	-1.28e-01	9.77e-03	-13.1
LatP										5.43e-03	2.63e-03	2.1
LatT										4.38e-02	4.77e-03	9.2
LongT										-1.12e-01	9.87e-03	-11.4
CP^2	-1.27e-02	4.84e-03	-2.6									
CT^2	-1.50e-01	2.45e-03	-61.2	-4.30e-01	5.89e-02	-7.3						
Age x CP	-1.07e-02	7.86e-04	-13.6	-1.09e-02	3.58e-03	3						
Age x CT	-1.92e-02	1.50e-03	-12.8	3.33e-01	1.44e-02	23.1	1.59e+00	1.21e-01	13.1			
CP x CT	9.58e-03	1.29e-03	7.4	7.45e-03	3.01e-03	2.5	8.11e-02	2.52e-02	3.2			
LatP x CT										-1.08e-02	1.74e-03	-6.2
LatP x LatT										4.15e-03	7.95e-04	5.2
LatP x LongT										-1.09e-02	1.61e-03	-5.3
CP x LongT										-2.63e-03	4.98e-04	-6.8
	r	R^2 M	R^2 C	r	R^2 M	R^2 C	r	R^2 M	R^2 C	r	R^2 M	R^2 C
	0.69	0.57	0.91	0.53	0.51	0.98	0.59	0.18	0.40	0.73	0.49	0.68

7. Summary statistics of two-trait models

Supporting Information Table S1.5. Statistics of random and fixed effects from linear mixed-effect models of the vertical growth-radial growth and vertical growth-leaf flushing two-trait models. Obs: number of trait measurements; Variance: variance explained by the random effects; SD: standard deviation of each level of random effects; Estimate: coefficient of the regression shown in logarithmic scale; SE: standard error of each fixed variable; t: Wald statistical test that measures the point estimate divided by the estimate of its SE, assuming a Gaussian distribution of observations conditional on fixed and random effects. Coefficients of the fixed effects of the model: Cov: trait covariate; CP: climate of the provenance origin; CT: climate of the trial; CP^2: quadratic effect of the climate of the provenance. Coefficients of the interactions: Age x CP, CP x CT, Cov x Age and Cov x CT. R^2M: percentage of the variance explained by the fixed effects (Marginal variance); R^2C: percentage of the variance explained by the random and fixed effects (Conditional variance); r: Pearson correlation. The trait co-variate (Cov) for growth-radial growth is radial growth and for vertical growth-leaf flushing is leaf flushing. The climate variable of the trial (CT) for the two-trait models is precipitation of the wettest month (BIO13). The climate variable of the provenance (CP) for the two-trait model is maximal potential evapotranspiration.
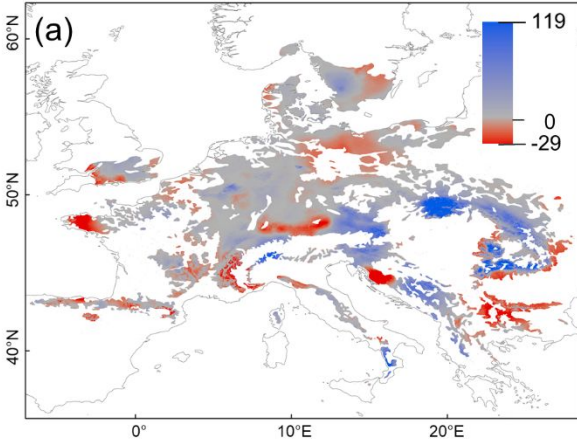
	Vertical growth-Radial growth			Vertical growth-Leaf flushing		
Model	Linear Mixed Effect			Linear Mixed Effect		
	Random Effects			Random Effects		
	Obs	Variance	SD	Obs	Variance	SD
Provenance	187	1.70e-03	4.21e-02	150	2.33e-02	1.53e-01
Trial	19	3.26e-02	1.81e-01	6	1.05e-01	3.24e-01
Trial:Block	56	2.20e-03	4.60e-02	17	1.00e-03	3.24e-02
Trial:Block:Tree	31339	9.50e-03	9.70e-02	10634	9.82e-02	3.13e-01
Residuals		1.50e-02	1.23e-01		2.70e-03	5.21e-02
	Fixed Effects			Fixed Effects		
	Estimate	SE	t	Estimate	SE	t
Intercept	4.38E+00	4.51e-02	97.18	4.94e+00	4.23e-01	11.68
Cov	3.50E-01	5.02e-03	69.72	6.24e-02	8.40e-02	0.74
Age	-1.97E-01	1.26e-02	-15.66	7.40e+00	5.28e-01	14.01
CP	5.04E-03	3.47e-03	1.45	2.59e-02	1.38e-02	1.87
CT	-1.33E-01	3.47e-02	-3.84	1.91e+00	3.89e-01	4.92
CP^2	-5.26E-03	2.43e-03	-2.17			
Age x CP				-1.96e-02	5.33e-03	-3.68
CP x CT	-3.47E-02	9.66e-03	-3.59	1.78e-02	5.72e-03	3.11
Cov x Age	1.05E-01	3.44e-03	30.57	-1.43e+00	1.09e-01	-13.08
Cov x CT	8.02E-02	3.82e-03	21	-3.84e-01	7.84e-02	-4.89
	r	R^2 M	R^2 C	r	R^2 M	R^2 C
	0.76	0.62	0.95	0.77	0.47	0.99

8. Differences in spatial predictions between future and current climate for one- and two-trait models

Vertical growth prediction for 12 year-old trees showed small changes in the core of the species range, and moderate decrease in growth in some areas of southern, eastern, western and northern Europe. Increases in vertical growth were mainly expected in the eastern region of the distribution (Supporting Information Figure S1.3a, Appendix S1). Radial growth of 12 year-old trees was predicted to increase in the eastern regions and to decrease across the rest of the range (Supporting Information Figure S1.3b, Appendix S1). Survival of 6 year-old trees was expected to strongly decrease in the western and southern parts of the distribution. Increases in young tree survival were mainly expected in central and some eastern regions of the species range (Supporting Information Figure S1.3c, Appendix S1). The model predicted later leaf flushing in the future than at present for almost all central and western parts of the species distribution. Earlier leaf flushing in the future than today was particularly expected in Sweden (Supporting Information Figure S1.3d, Appendix S1). Differences in vertical growth predictions between future and present climatic conditions for the vertical growth-radial growth model showed an overall increase in vertical growth in some regions of the eastern and southern range; the largest decrease was expected in the southeastern region (Supporting Information Figure S1.3e, Appendix S1). Differences in vertical-growth predictions between the future and present conditions for the vertical growth-leaf flushing model anticipated a decrease in the southeastern and the southern range. A small increase in the northeast was predicted by this model (Supporting Information Figure S1.3f, Appendix S1).
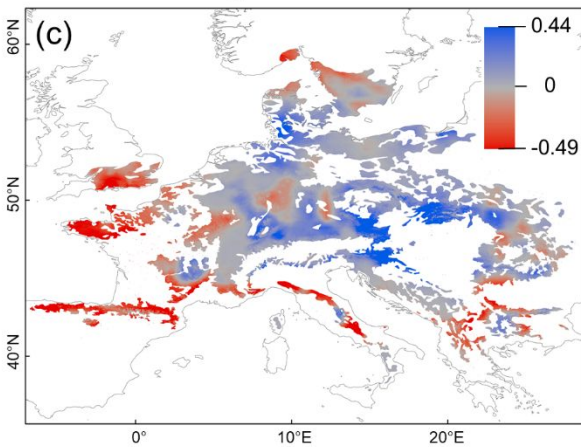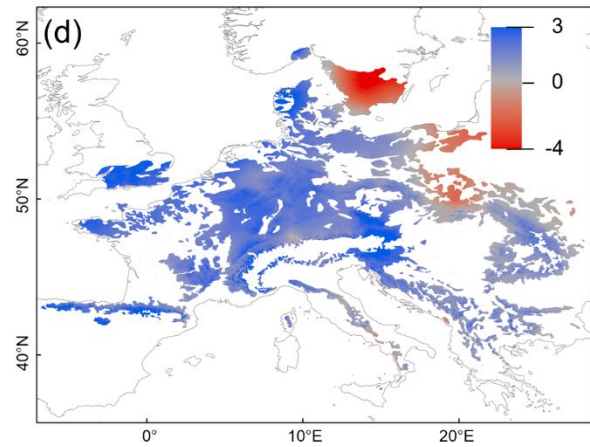
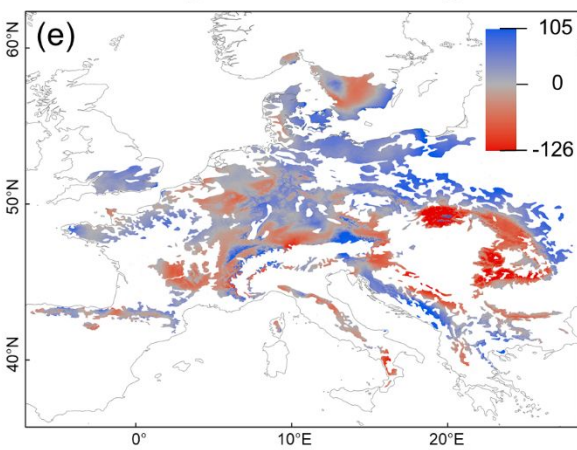**Supporting Information Figure S1.3.** Differences in predictions between future (2070) and contemporary (2000-2014) climate for one-trait models in beech range: (a) vertical growth of 12 year-old trees (in cm); (b) radial growth of 12 year-old trees (in mm); (c) probability of young tree survival of 6 year-old trees; (d) leaf flushing of 12 year-old trees (difference in Julian days); and for two-trait models: (e) vertical growth (in cm; co-variate radial growth) and (f) vertical growth (in cm; co-variate leaf flushing). The color gradient depicts the clinal variation from low (red) to high (blue) values.

1
2
3 Dear Editors,
4
5
6
7 Many thanks again for the review, we addressed all the minor points raised by the editors and
8 one of the reviewers.
9
10
11
12 Yours sincerely,
13
14
15
16 Marta Benito Garzón on behalf of the co-authors
17
18
19
20 EDITOR'S COMMENTS TO AUTHORS
21 Editor: Blonder, Benjamin
22 Comments to the Author:
23 The authors have assessed the substance of all of the reviewers' and my points. The work is
24 likely to be of broad interest to our readership. I think the manuscript is essentially ready to go.
25 There are only a few minor presentation issues remaining that could be trivially addressed by the
26 authors:
27
28
29
30 R: Many thanks for checking and editing the manuscript, we followed all your advises in our
31 reviewed version of the manuscript.
32
33
34
35 Abstract: I would rather say that one of the main conclusions is that the drivers of range limits are
36 dependent on trait x environment interactions - not only do multiple traits matter, but each trait
37 matters differently depending on the environmental variable.
38 R: Thank you, we agree and changed the sentence accordingly.
39
40
41
42 103: broadleaf, not broadleaved
43 R: Changed
44 221: delta term is not clear, suggest replacing with ∆AIC
45 R: Changed
46 488: based on, not based in
47 R: Changed
48 506: this is a run-on sentence - please fix.
49 R: We split this sentence in two.
50 510: could, not can

Changed

Figure 1: can you make symbols in the inset legend larger? They are hard to see.

We made larger the symbols of the inset, thank you.

Figure 2/4: please consider replacing color scales with more colorblind-friendly version, e.g. just a simple red-gray-blue gradient (no yellow or green)

R: Thank you, we changed them to a red-gray-blue scale.

Referee: 2

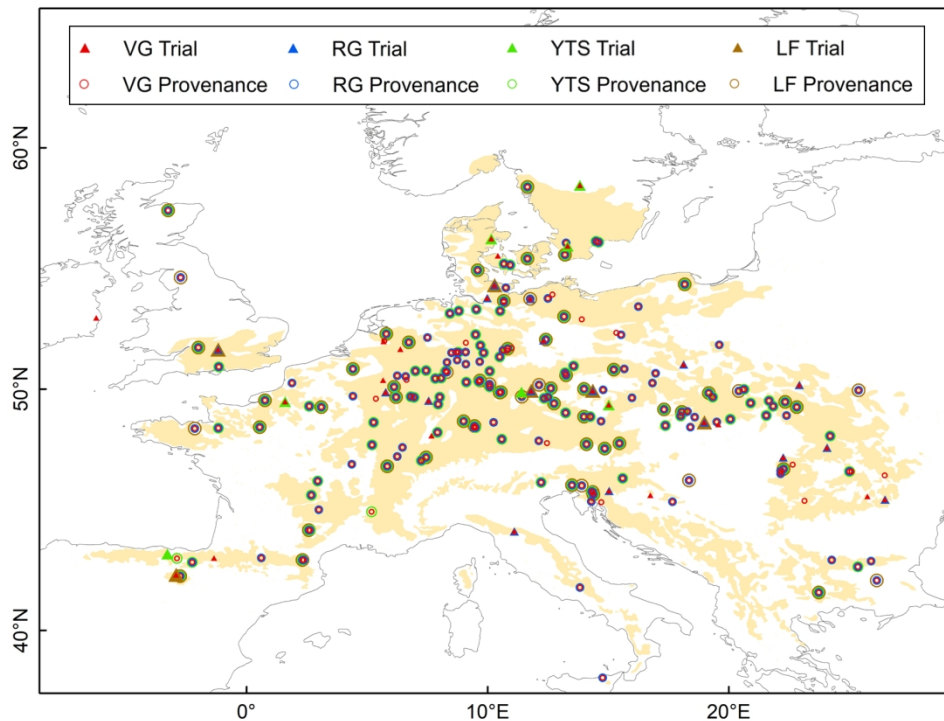I am happy that my comments were useful for this manuscript. Just a note, in this sentence: "[...in certain parts of the southern and eastern range of beech, reflecting the climatic marginality due to continentality of the species in these areas...]", you perhaps refer to continentality of the climate, and not of the species.

R: Thank you, we fixed it.

	VG	RG	YTS	LF	H-RG	H-LF
Measurements	203 105	34 237	41 309	7 863	34 237	12 087
Trees	108 415	31 339	37 433	7 863	31 339	10 634
Trials	36	19	7	7	19	6
Provenances	205	186	114	62	186	150
Age	2 to 15	8 to 15	2 to 6	12	8 to 15	6, 9, 11, 12, 15

Figure 1. Map: Distribution range of Fagus sylvatica L. (shaded in beige) and location of the provenances and trials by trait. Circles indicate the location of the provenances and triangles that of the trials. Different colors have been employed to indicate the different traits (VG: vertical growth; RG: radial growth; YTS: young tree survival; LF: leaf flushing). Table: The extent of data from the BeechCOSTe52 database (Robson et al. 2018) used for modelling. Measurements: total number of measurements; Trees: total number of individual trees; Trials: total number of trials; Provenances: total number of provenances, Age: the age at which the trees were measured. Columns indicate sample sizes for the traits used in the one-trait models and in the two-trait models.
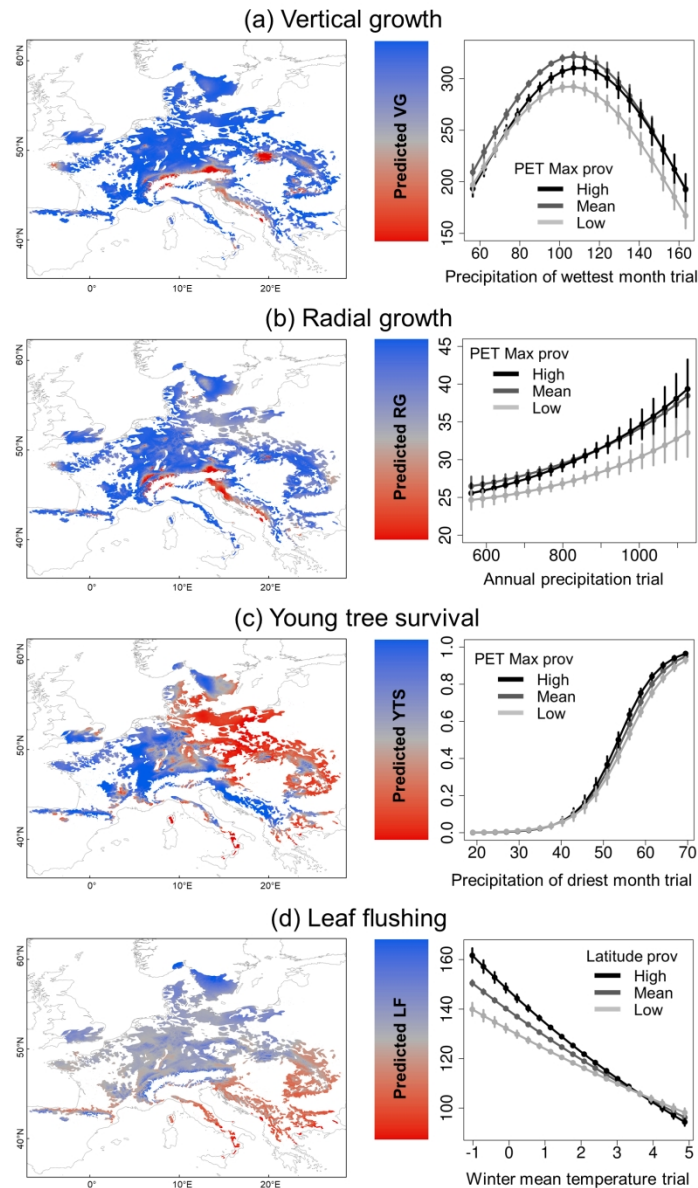
160x160mm (300 x 300 DPI)

Figure 2. Spatial projections for (a) vertical growth (cm), (b) radial growth (mm), (c) young tree survival (probability) and (d) leaf flushing (Julian days) generated using one-trait models (maps on the left), and corresponding graphs of interactions between the best environmental predictor variable across the trials divided according to environment at the provenance for each of the four traits (graphs on the right). Interactions represent the differences in trait values that can be attributed to the provenance (interpretable as local adaptation driven by PET max in (a), (b), and (c) and driven by the latitude in (d)). Interactions also represent the differences in trait values that can be attributed to the environmental conditions of trial (interpretable as phenotypic plasticity driven by the environmental variables shown in the x-axis). Black, dark grey, and light grey lines represent high, medium and low values of the climatic variable of the provenances (as opposed to those of the trial, indicated on the x-axis). The vertical lines represent the confidence intervals. The maps display the trait projection for contemporary climate (inferred from 2000-2014 meteorological data) across the current species range. The color gradient depicts the clinal variation from low (red) to high (blue) values of each trait. The values of the different traits are represented in the following way: vertical growth (cm), radial growth (mm), probability of young tree survival (0 =dead,

1
2
3
4
5
6
7
8
9
10
11
12
13
14
15
16
17
18
19
20
21
22
23
24
25
26
27
28
29
30
31
32
33
34
35
36
37
38
39
40
41
42
43
44
45
46
47
48
49
50
51
52
53
54
55
56
57
58
59
60

1=alive) and leaf flushing (Julian days). PET max prov: maximal monthly potential evapotranspiration at the provenance; Latitude prov: latitude of the provenance.
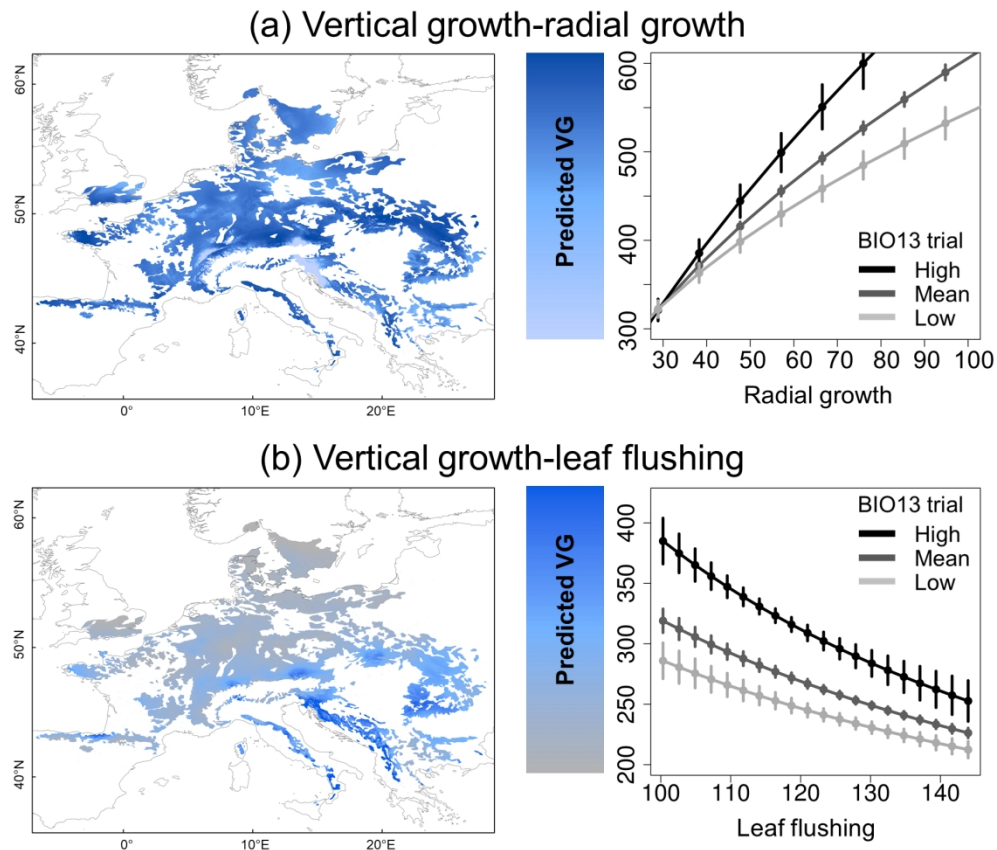
135x230mm (300 x 300 DPI)

Figure 3. Spatial projections of vertical growth (cm) for (a) Vertical-radial growth model and (b) vertical growth-leaf flushing models (maps on the left), and the corresponding graphs of co-variation between vertical growth and the covariate: (a) DBH (mm) and (b) leaf flushing (Julian days). Black, dark grey, and light grey lines represent high, medium and low values of the precipitation of the wettest month of the trial (BIO13). The vertical lines represent the confidence intervals. The maps display the trait projection for contemporary climate (inferred from 2000-2014 meteorological data) across the current species range. The color gradient depicts the clinal variation in vertical growth from 200 cm (gray) to 600 cm (blue).
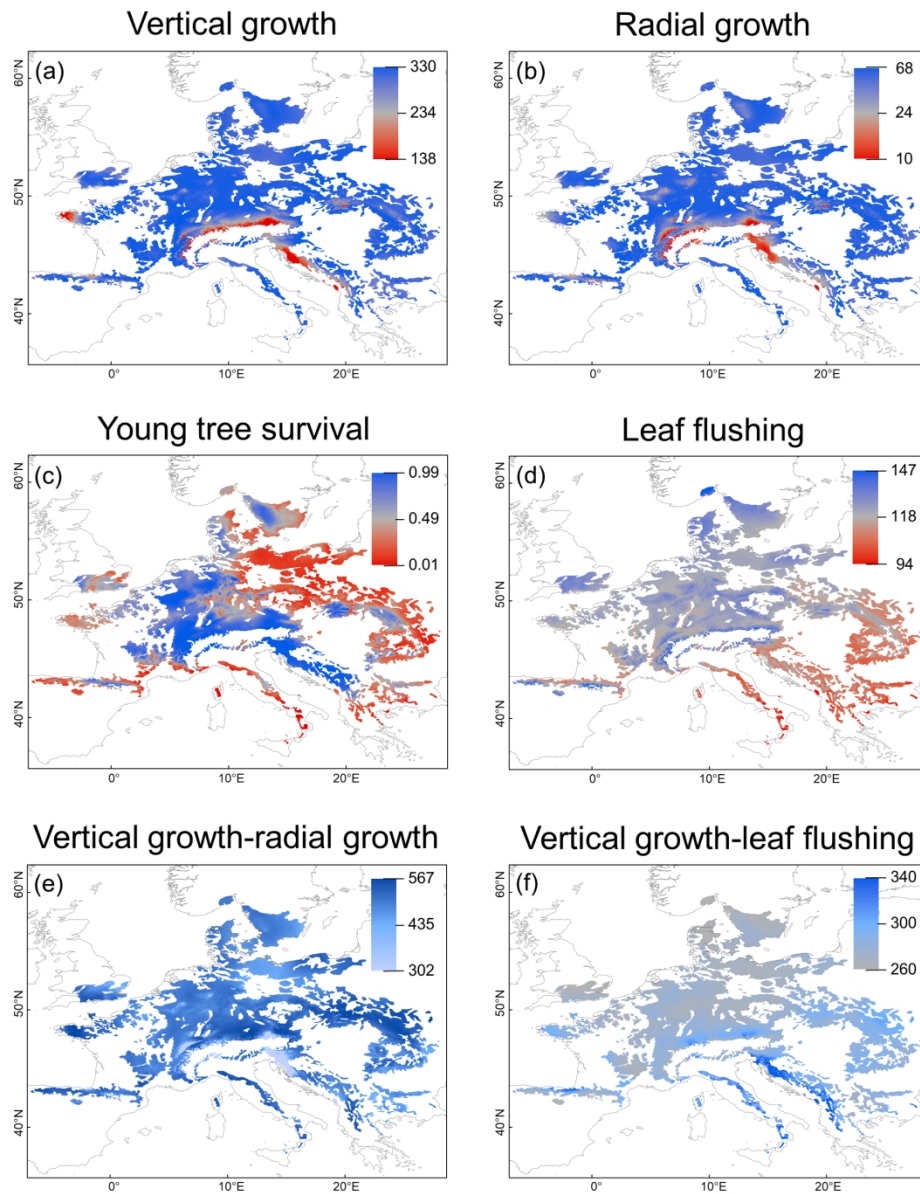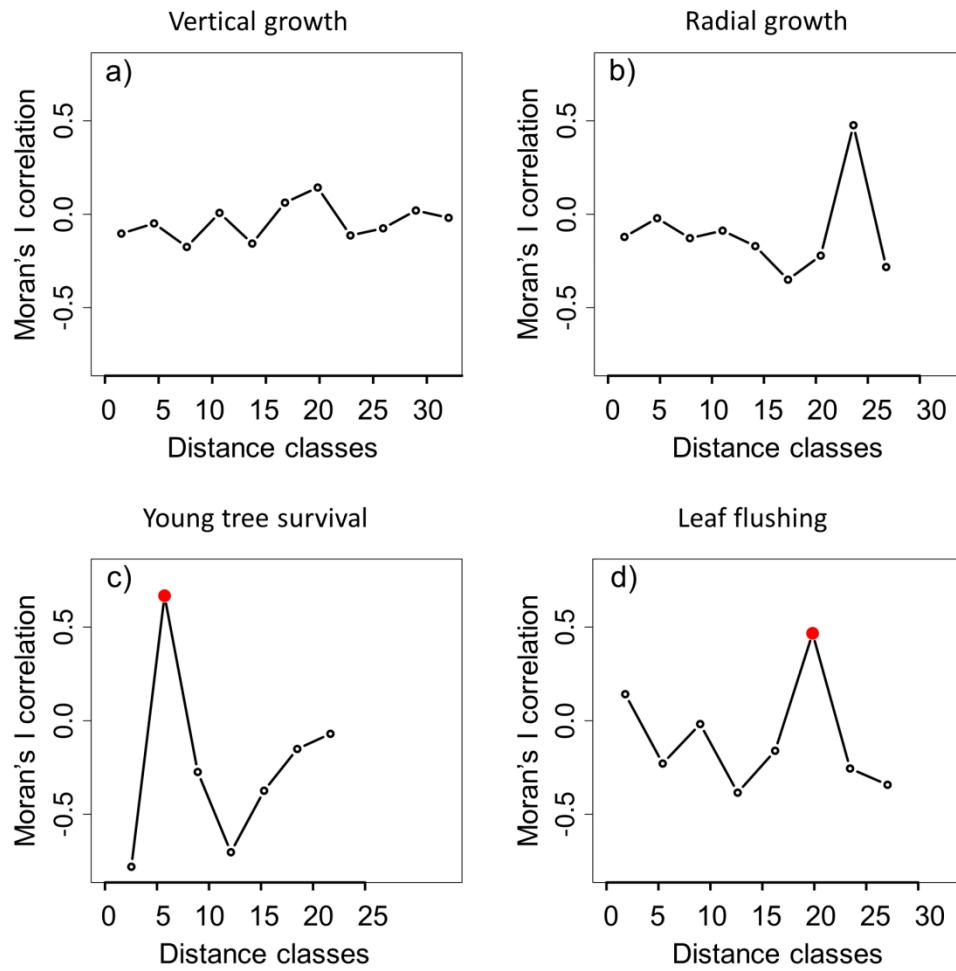
160x137mm (300 x 300 DPI)

Figure 4. Spatial predictions for 2070 (RCP 8.5) across the species range for one-trait models: (a) vertical growth (cm); (b) radial growth (mm); (c) probability of young tree survival (0=dead; 1=alive); (d) leaf flushing (Julian days); and for two-trait models: (e) vertical growth (cm; co-variate radial growth) and (f) vertical growth (cm; co-variate leaf flushing). The color gradients depict the clinal variation from low (red) to high (blue) values.

165x209mm (300 x 300 DPI)

Supporting Information Figure S1.1. Correlograms of Moran's I correlation coefficient (y-axis) and the distance classes (x-axis) for vertical (a) and radial (b) growth, young tree survival (c), and leaf flushing (d). Moran's correlation coefficient ranges between 1 and -1. Distance classes are Euclidian and in degrees. Distances of significant spatial dependence are shown in red (significant values $p < 0.05$).
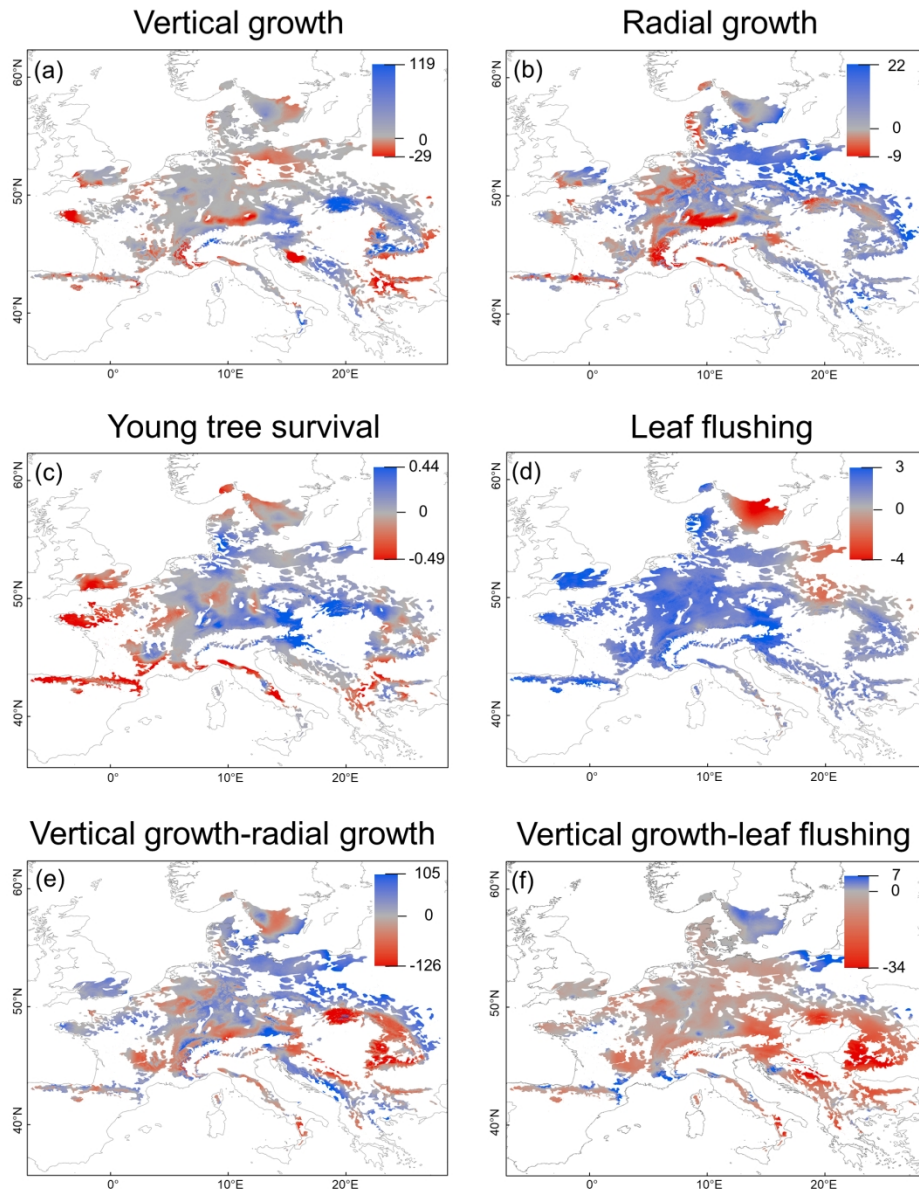
160x157mm (300 x 300 DPI)
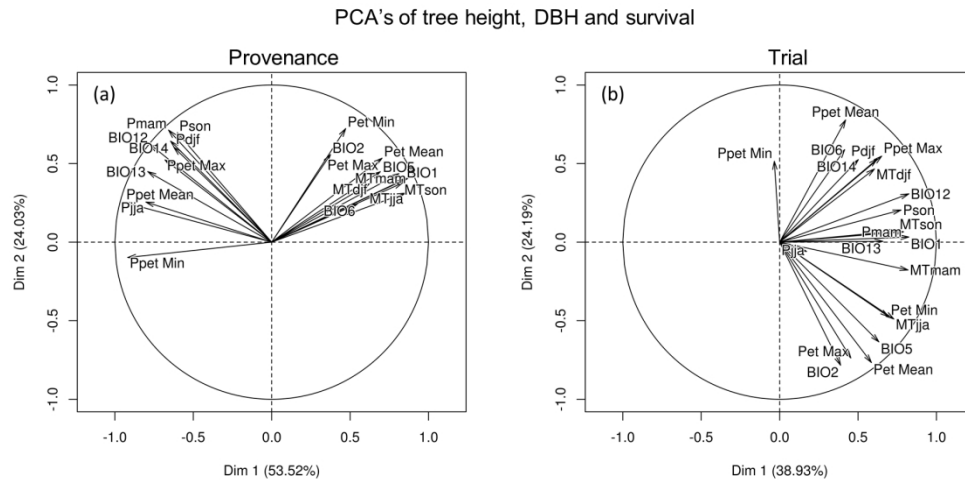
1
2
3
4
5
6
7
8
9
10
11
12
13
14
15
16
17
18
19
20
21

PCA's of tree height, DBH and survival

Supporting Information Figure S1.2. Results of PCA for checking for co-linearity and reducing the climatic space to select the final climate variables for the stepwise procedure used in the models on traits vertical and radial growth, and young tree survival, conducted by provenance (a) and by trial (b). When two variables are strongly correlated, only one of them was used in models. The variance explained by the first two axes is indicated in the figures.

160x80mm (300 x 300 DPI)

22
23
24
25
26
27
28
29
30
31
32
33
34
35
36
37
38
39
40
41
42
43
44
45
46
47
48
49
50
51
52
53
54
55
56
57
58
59
60

Supporting Information Figure S1.3. Differences in predictions between future (2070) and contemporary (2000-2014) climate for one-trait models in beech range: (a) vertical growth of 12 year-old trees (in cm); (b) radial growth of 12 year-old trees (in mm); (c) probability of young tree survival of 6 year-old trees; (d) leaf flushing of 12 year-old trees (difference in Julian days); and for two-trait models: (e) vertical growth (in cm; co-variate radial growth) and (f) vertical growth (in cm; co-variate leaf flushing). The color gradient depicts the clinal variation from low (red) to high (blue) values.

165x209mm (300 x 300 DPI)